Resonant Magnetization Tunneling in Molecular Magnets

Jonathan R. Friedman
Department of Physics
Amherst College
Amherst, MA 01001-5000

The frontier between the classical and quantum worlds can be approached in one of two ways: from the top down or the bottom up. The top-down approach entails starting with an essentially classical variable (e.g. the flux in a superconducting loop, the charge on a small superconducting island or the magnetization of a single-domain magnetic particle) and squeezing down the size of the system (thereby increasing the energy-level separations) until the variable begins to behave quantum mechanically. Most of the chapters in this book involve this approach in some form or another. The alternative, bottom-up approach begins with microscopic quantum objects (like individual ions or spins) and groups them together into somewhat more complex objects in an attempt to see when and how quantum behavior crosses over to classical.

Magnetic molecules, the subject of this chapter, fall into this latter category. They are the agglomeration of a handful of magnetic ions, whose spins are so strongly bound together by the exchange interaction that at low temperatures they act as a single macrospin. In many ways they behave like classical magnets in that they exhibit magnetic hysteresis at sufficiently low temperature. At the same time, these hysteresis loops show unmistakable evidence of quantum tunneling in the form of steps at regular intervals of magnetic field, as will be discussed in detail below. This dual behavior indicates that these magnets straddle the fence between the quantum and classical worlds, and not only because they are mesoscopic in size, containing only a handful of constituent objects. Notably, molecular magnets can relax via a hybrid process that mixes quantum tunneling with thermal relaxation. This result is something of a surprise since much of the original (semiclassical) theoretical work on tunneling in macroscopic systems predicted that as temperature is raised there should be a crossover between purely quantum relaxation and purely thermal (over-barrier) relaxation. At temperatures well above the so-called crossover temperature T_c, the system is expected to relax only by thermal activation [1-3]. In many ways the molecular magnets, in which the spin is of order 10, are fairly well described by the semiclassical theories. However, the finite size of the spin allows the observation of the hybrid thermal-quantum process illustrated in Fig. 1. Thus, tunneling effects can be observed in the molecular magnets at temperatures well into the regime in which semiclassical theories would predict purely thermal dynamics.

In some respects, the study of quantum phenomena in magnetic particles and molecules is richer than in most other systems of current interest. In particular, tunneling in magnetic systems can be produced by a variety of mechanisms that can be distinguished from one another by selection rules associated with each mechanism. In most systems it is a rather trivial question to ask, "What causes tunneling?" In fact, many physicists, when first asked this question, rightly react as if they had been asked, "Why are there physical laws?" This is because, for most systems, tunneling follows in a straightforward manner from the basic laws of quantum mechanics. These systems, which I will call particle-like, have Hamiltonians of the form $\mathcal{H} = \frac{p^2}{2M} + V(x)$. The dynamical variable here, x, could be a Cartesian coordinate, e.g. the position of the center of mass of a particle, or it could be a coordinate in more abstract space, e.g. the flux in a SQUID. The

potential in cases of interest has at least one metastable minimum, p is momentum conjugate to x (e.g. the charge difference across the Josephson junction(s) of a SQUID) and M an effective "mass". The "cause" of tunneling, then, is simply that x is not a conserved quantity because x and p do not commute. That is, kinetic energy lies at the root of tunneling. The only way to "turn off" tunneling is to take $M \to \infty$. But, in doing so, the density of levels becomes quasicontinuous and the system becomes classical. Therefore, a quantum system with a particle-like Hamiltonian must have tunneling.

In contrast,* spin systems have no explicit kinetic degrees of freedom. The simplest Hamiltonian for a spin with easy-axis anisotropy takes the form

$$\mathcal{H} = -DS_z^2 - g\mu_B S_z H_z + \mathcal{H}', \tag{1}$$

where the second term represents the Zeeman coupling between the spin and a magnetic field and $\mathcal{H}$ contains all terms that do not commute with S_z. Now, unlike in the particle-like case, it is possible for a spin to remain quantum (having well-separated energy levels) and have $\mathcal{H}' \to 0$. In this limit, S_z is a conserved quantity and no transitions between eigenstates of S_z are allowed: Tunneling can be turned off without the spin becoming classical. So, it is meaningful to ask here "What causes tunneling?" $\mathcal{H}'$ could include a transverse magnetic field or a transverse anisotropy or, perhaps, something more exotic. Because different mechanisms have different symmetries, it is possible to determine the dominant tunneling mechanisms by looking for tunneling selection rules associated with the symmetry. This will be discussed in more detail later in this chapter.

I.A. Macroscopic Quantum Tunneling in Magnetic Systems

The field of molecular magnetism has grown immensely in the last few years and it would be impossible to adequately review every facet of it in this chapter. Instead I will focus primarily on experimental results for the most studied of the molecular magnets, Mn_{12}–Acetate (from hereon called simply Mn_{12}). In Section II I will review the work done at the City College of New York (in collaboration with researchers at the University of Barcelona and at Xerox Corporation) that became the first unambiguous evidence for resonant magnetization tunneling in magnetic systems [4-7]. (The work of other groups is reviewed in [8, 9].) I will show how the data can be explained with a simple spin Hamiltonian, which has now been confirmed and refined by several spectroscopic studies [10-14]. In Section III, I will turn to the question of "What causes tunneling?" and show that, at least for Mn_{12}, the tunneling is driven in some part by a transverse magnetic field, presumably of hyperfine origin. I will also review the theoretical picture of thermally assisted resonant tunneling and discuss experiments that elucidate the different roles played by dipole and hyperfine fields in the relaxation. Section IV will focus on some recent results, including experiments on the molecular magnet, "Fe_8", in which the tunneling rate can be markedly suppressed by a geometric-phase effect controlled by a magnetic field.

* The fundamental difference between particle-like systems and spin systems is the structure of their respective Lie algebras. The commutator for a particle-like system $[x, p] = i\hbar$ is a c-number. For a spin system, on the other hand, the commutator, $[S_i, S_j] = i\varepsilon_{ijk} S_k$, which is an operator. Thus, there is no way to rigorously map one system onto the other.

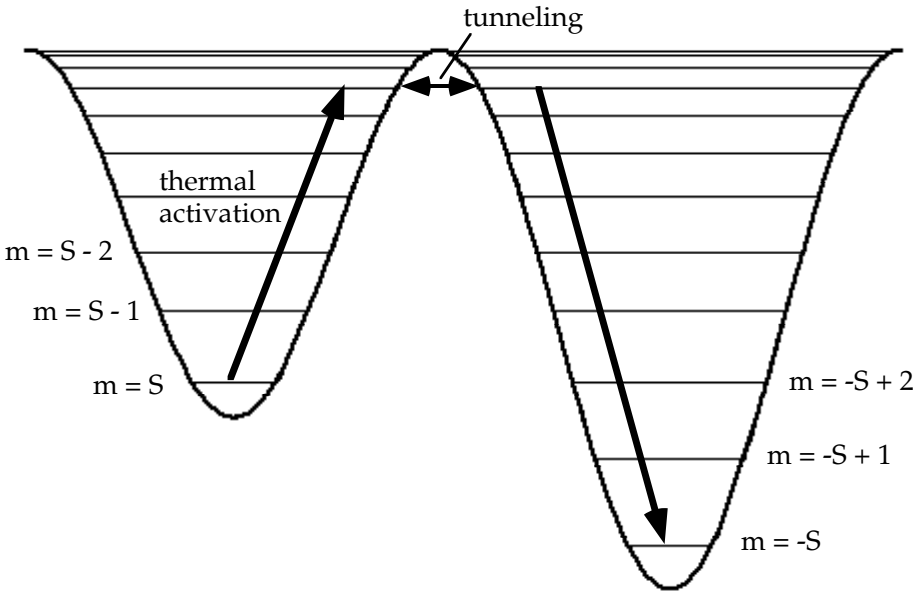

Fig. 1 Double-well potential of a uniaxial spin. One well corresponds to spin up, the other to spin down and an applied field tilts the potential. The different $|m\rangle$ levels for an $S = 10$ system are shown. The arrows schematically illustrate the thermally assisted resonant tunneling process described in the text.

The concept of quantum tunneling is almost as old as quantum mechanics itself. The ability of a particle to traverse a classically forbidden region has become ubiquitous in physics: an alpha particle decaying out of a nucleus, electron-hopping conduction in insulators, Cooper pairs tunneling through a Josephson Junction, etc. In the late 1970's and early 1980's, Caldeira and Leggett [15, 16] developed the formal theory of macroscopic quantum tunneling, which predicted that under suitable circumstances macroscopic objects, consisting of many (thousands, millions or billions of) microscopic entities strongly coupled together, could exhibit uniquely quantum-mechanical properties. The first clear experimental evidence for macroscopic quantum tunneling was provided by Clarke, et al. [17], who showed that in a Josephson Junction the phase of the superconducting order parameter across the junction can tunnel from a "superconducting" zero-voltage state to a "normal" finite-voltage state. That research is described in detail in the chapter by Devoret et al. in this volume.

The possibility of quantum tunneling of magnetization was first suggested in 1959 by Bean and Livingston [18], who found that in the superparamagnetic systems they were studying some particles seemed to remain unblocked even at the lowest temperatures. This interpretation was later put forth to explain anomalous relaxation phenomena discovered at low temperatures in other magnetic systems [19-25]. Guided by the work of Caldeira and Leggett [3, 15, 16], important theoretical progress was made in the late 1980's [26-28] and much of the theoretical work on the subject is reviewed in [29-32] as well as in Braun's contribution to this book.

The semiclassical concept of tunneling usually involves the notion of a particle that escapes from a metastable potential well without having sufficient energy to overcome the potential barrier: instead of climbing over the barrier, it "tunnels" through it. The tunneling of the magnetization vector in a small magnetically ordered particle differs somewhat from this picture in that the tunneling occurs in angular space with the magnetization vector rotating from one potential minimum to another. Let us consider a single-domain particle of sufficiently small size

(smaller than the domain-wall width) that it can be treated as a single, large spin. Further, we assume that the exchange interactions between the spins within the particle are so strong and the temperature is so low that the internal degrees of freedom (magnons) can be neglected. The presence of anisotropy gives the magnetization vector a preferred direction, the easy axis. The Hamiltonian most relevant for the systems to be discussed in this chapter is

$$\mathcal{H} = -DS_z^2 - AS_z^4 - g\mu_B S_z H_z + \mathcal{H}' \tag{2}$$

where D and A are the anisotropy constants originating primarily from crystal and molecular fields; as in Eq. (1), $\mathcal{H}'$ contains terms that do not commute with S_z and is thus responsible for tunneling. In this model, the easy axis is the z axis. In the absence of a magnetic field, the magnetization has two equivalent energy minima, corresponding to being aligned parallel or antiparallel to the z axis. In order to switch from one minimum to another, the system must overcome an energy barrier of $U = DS^2 + AS^4$. The height of the barrier can be reduced by the applied field. The potential energy for this system is shown schematically in Fig. 1, where the asymmetry is produced by an external field and the levels correspond to the magnetic quantum numbers m, the eigenvalues of S_z. At high temperatures, the magnetization is easily thermally activated over the barrier and remains in one well for a time much shorter than typical measurement times. Thus, it behaves like a paramagnet and, being a large-spin object, is dubbed a "superparamagnet."

The rate for making a thermal transition from one well to the other is described by an Arrhenius law, $\Gamma = \omega_0 \mathrm{e}^{-U/kT}$, where ω_0 is called the attempt frequency and represents the frequency of small oscillations in the metastable well. When the temperature is reduced below a certain temperature (the so-called blocking temperature), there is insufficient thermal energy to induce transitions over the barrier on the timescale of a typical measurement and the system is said to be "blocked," or trapped in one well or the other. Transitions between wells can still be observed, but their rate is slow compared to the measurement time. In the limit of zero temperature, the system can only relax via tunneling. As mentioned above, the semiclassical picture predicts that as the temperature is raised through T_c, the system should cross over from this zero-temperature-tunneling behavior to simple thermal activation. This should occur when the Arrhenius exponent and WKB tunneling exponent are nearly equal.

In order to observe macroscopic manifestations of quantum-mechanical effects, dissipation must be low. The theory of Caldeira and Leggett [3, 15, 16] demonstrates that if one can treat the environment as a set of independent harmonic oscillators linearly coupled to the macroscopic object, then the effect of dissipation is to add a term to the WKB exponent, decreasing the tunneling rate. This effect will not destroy tunneling if the sources of dissipation are infrared-weak, i.e. have a small spectral weight at low frequencies. For, they showed, it is the low-frequency environmental factors that contribute most to dissipation. Phonons are in fact infrared weak since, according to the Debye model, the spectral density for acoustic phonons of frequency ω is proportional to ω^3. Garg and Kim [33, 34] have shown in detail that phonons have little dissipative effect on the tunneling of magnetization. Very general arguments [29] indicate that electrons in metallic particles can be a significant source of dissipation and so tunneling is generally sought in insulating materials.

Experimental evidence for quantum tunneling of magnetization has been found in many materials at low temperatures. Many of these studies have been reviewed [32, 35-39]. For most of these studies, samples consisted not of magnetic particles with a unique energy barrier, but, rather, of particles having a broad distribution of energy barriers so that only statistical quantities of the whole distribution could be studied. In a variety of these systems the magnetic relaxation rate is found to cross over to a temperature-independent regime at low temperatures. This temperature-independent "magnetic viscosity" is cited as evidence for quantum tunneling. However, because most of these systems cannot be precisely characterized, no rigorous comparison between theory and experiment is possible.

It was thus very desirable to obtain samples containing magnetic clusters that are closely monodispersed. One way of doing this is to study not an ensemble of particles but a single, well-characterized particle. This approach is discussed in Wernsdorfer's chapter in this volume.

Experimental evidence for tunneling has been reported by Awschalom and coworkers [38], who observed a resonance in the ac susceptibility and noise spectrum of horse-spleen ferritin at very low temperatures; they attributed this to quantum coherent tunneling of the magnetization vector between two degenerate orientations in a double-well potential. These results have received much attention, but have also elicited considerable debate [40-44].

The molecular magnets are ideal systems to study magnetization tunneling. Unlike most ensembles of magnetic clusters, the magnetic subunits of a molecular crystal have unique, chemically determined properties: a macroscopic sample of a molecular magnet is comprised of about 10^{17} nominally identical entities with the same magnetic properties and characteristic energies. Another important feature of these systems is that while the spin of each cluster, $S \approx 10$, is large for a molecular system, it is small relative to most superparamagnetic systems. This small spin value together with the system's large magnetocrystalline anisotropy yields an appreciable energy separation between spin levels, allowing the observation of a novel physical effect: resonant spin tunneling between matching levels on opposite sides of a potential barrier. In the remainder of this chapter, I will focus exclusively on the evidence for such tunneling in molecular magnets, particularly Mn_{12}.

I.B. Background on Mn12

$Mn_{12}O_{12}(CH_3COO)_{16}(H_2O)_4$ was first synthesized by Lis [45] in 1980. He found that the compound contains four Mn^{4+} (S = 3/2) ions in a central tetrahedron surrounded by eight Mn^{3+} (S = 2) ions in a non-coplanar ring, as shown in Fig. 2. The Mn ions are strongly superexchange-coupled through oxygen bridges. Surrounding this central magnetic core are 16 acetate ions and 4 water molecules per molecular cluster. These molecules crystallize into a body-centered tetragonal lattice with the c axis having the smallest lattice parameter. Magnetic interactions between molecules are thought to be small both because the nonmagnetic ligands keep Mn ions of different clusters far apart (> 7Å) [45] and because the Curie-Weiss temperature for this system is <70 mK [46-49]. In contrast, the coupling between Mn ions within a cluster is so strong that at low temperatures the system can be treated as a single macrospin with $S = 10$.[*]

[*] Inelastic neutron scattering experiments [50] indicate that excitations to other (e.g. $S = 9$) spin manifolds occur at energies of ~30 K. Because of this, there has been some effort to theoretically treat the Mn_{12} molecule using a more complete multispin analysis [51-53]. While such a model predicts somewhat different tunnel splittings than a single-

Significant interest in Mn_{12} was created in 1991 when chemists at the University of Florence, Italy, discovered [54] that the compound had an unusually high spin ground state of S=10. This was determined by AC susceptibility measurements in zero DC magnetic field and confirmed by measurements of the DC saturation magnetization. The spin value suggests a simple picture (Fig. 2) of the spin order within a molecule, with all of the spins of one valence pointing up and the remainder pointing down [54-56]. This picture has recently been confirmed experimentally by polarized neutron diffraction studies [57] and theoretically by electronic-structure calculations [58]. Early electron-spin-resonance (ESR) experiments also indicated that Mn_{12} has a large negative magnetocrystalline anisotropy [54, 55]. This fact manifested itself in measurements the imaginary part of the AC susceptibility [47, 48, 54, 55], and in the hysteresis at low temperatures [59, 60]. This was essentially the first evidence that a microscopic magnet could exhibit one of the telltale signs of bulk magnets, namely, magnetic bistability. Unlike bulk magnets, however, where hysteresis is associated with the motion of domain walls, the hysteresis in Mn_{12} has been associated with the intrinsic bistability of the individual magnetic clusters [59]. Specific-heat measurements showed that no phase transition accompanies the onset of hysteresis [47, 48], confirming that the hysteretic behavior is associated with superparamagnetism, not long-range order. AC susceptibility data as well as DC magnetic relaxation data have indicated a single characteristic relaxation time [36, 46-49, 59-61] that obeys an Arrhenius law down to 2.1 K. This indicates that this system is close to an ideal superparamagnet: a collection of identical magnetic entities with the same orientation and energy barrier.

From fits of the relaxation time to the Arrhenius law, the barrier height has been found [36, 46-49, 59, 60, 62, 63] to be ~70 K and the attempt frequency is estimated to be $\sim 10^7$ Hz, which is unusually small for superparamagnetic systems. A number of early experiments provided possible evidence for temperature-independent quantum tunneling at low temperatures in Mn_{12}. Using small single crystals, Barbara et al. [36] and Paulsen et al. [46, 49] found deviations below 2.0 K from Arrhenius-law behavior toward a temperature-independent relaxation rate. Much of their conclusions were based on relaxation experiments that sometimes lasted several days and, nevertheless, probed only a small fraction of the total decay of the moment.

The first evidence for resonant tunneling in Mn_{12} came in 1995. Barbara et al. [36] found a minimum in the relaxation time $\tau(H)$ at $H = 0$, followed by a maximum at ~ 2 kOe. For a classical magnet, on the other hand, one expects the relaxation time to decrease monotonically with increasing field since the field reduces the energy barrier. They suggested that the increased tunneling rate at zero field may be due to "the coincidence of the level schemes of the two wells." At about the same time, Novak and Sessoli [48] found a similar minimum at $H = 0$ and another one at approximately 3 kOe. This rather limited data prompted them to make the remarkable conjecture that the observed behavior could be due to thermally assisted tunneling between excited states in a double-well potential. Despite the fact that the 3 kOe minimum they reported is not one of the fields at which resonant tunneling was later found to take place, their conjecture turned out to be correct, as we shall see below.

---

spin picture, the difference is not within the current experimental resolution. Furthermore, the data presented herein is currently quite adequately explained within the single-spin model.

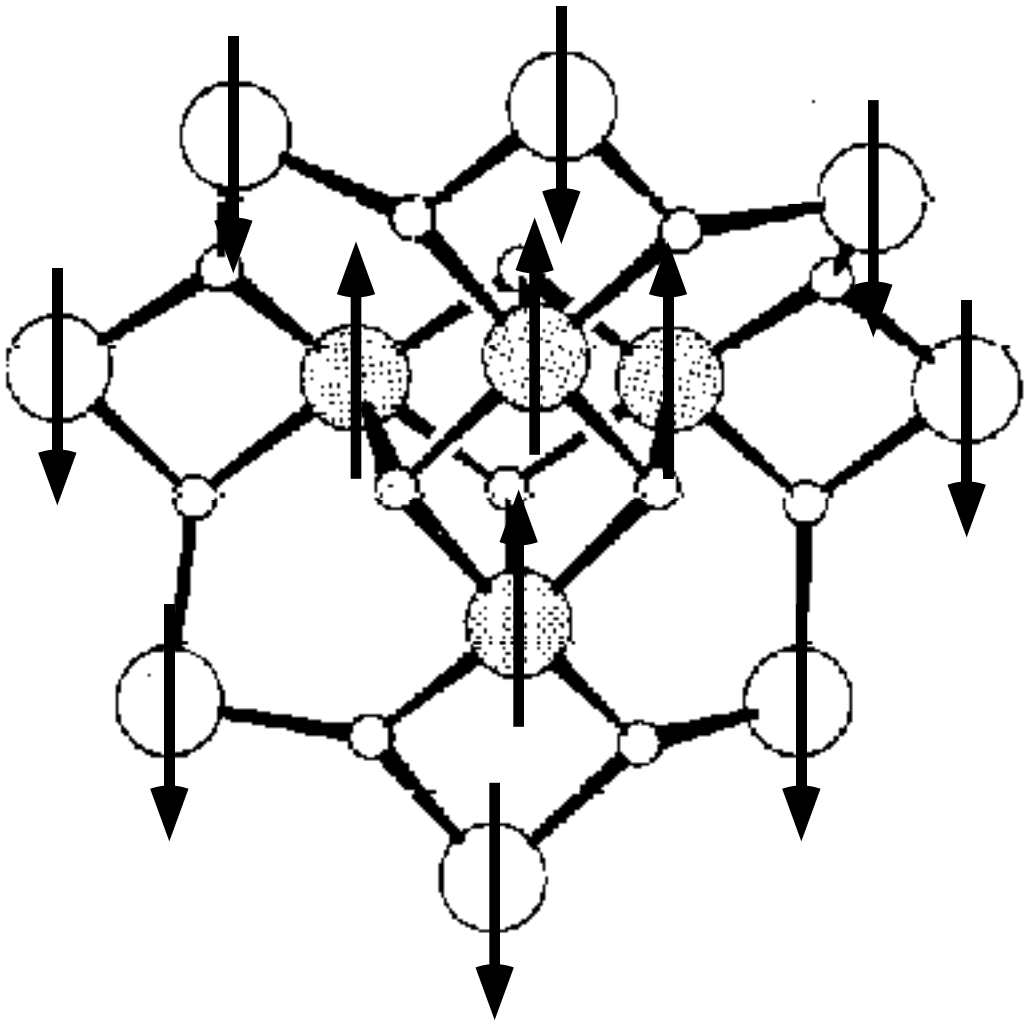

Fig. 2 Structure of magnetic core of the Mn_{12} molecule. Only the Mn^{4+} (large shaded circles), Mn^{3+} (large open circles) and oxygen (small circles) ions are shown. The arrows indicate the configuration of the spins that results in a total spin of 10 for the molecule. (Adapted from [59]).

II. EVIDENCE FOR THERMALLY ASSISTED RESONANT TUNNELING IN MN_{12}

In this section I will present magnetization data that demonstrate that Mn_{12} exhibits resonant magnetization tunneling between spin states, a phenomenon that has been confirmed through numerous experimental studies [5, 62, 64-70]. Before discussing the data, a few words about the samples are in order. While some of the data shown below were taken using millimeter-size single crystals, much of it comes from oriented powders of micron-size crystallites. Oriented-powder samples were prepared by the following (or similar) procedure. Approximately 10 mg of powdered sample was mixed into a low viscosity liquid such as melted paraffin, toluene or Stycast 1266, a non-magnetic epoxy. The liquid/sample mixture was poured into a sample container and placed in a 55-kOe magnetic field at room temperature. Because the crystallites are needle-like, with an aspect ratio as large as 10, their shape anisotropy induces them to torque to

align with the applied field. When an epoxy matrix was used, the system was kept at room temperature until the epoxy had set. Samples in paraffin and toluene matrices could be cooled down almost immediately. This resulted in pseudo-single-crystal samples in which all of the crystallites were oriented to within a few degrees of the field axis. Once the sample was cooled, the matrix held the crystallites fixed and prevented them from rotating when the field was changed during the measurements.

Fig. 3(a) shows the magnetization as a function of magnetic field at temperatures between 1.7 K and 3.0 K from a sample in a paraffin matrix. This data was obtained with the magnetic field applied along the easy axis of the sample. As expected for superparamagnetic systems, the area enclosed within the hysteresis loops is found to increase as the temperature is reduced. But, unlike typical superparamagnets, the hysteresis loop shows steps at certain values of magnetic field. As one proceeds around the loop, steps occur as the magnetic field is increased from zero, but no noticeable steps occur when the field is reduced back to zero.

It should be reiterated that the hysteresis observed in this system is a manifestation of the bistability of the individual Mn_{12} molecules, not the motion of domain walls since there are no domains in the system. The hysteresis is instead attributed to the fact that each magnetic entity has an energy barrier to magnetization reversal and can therefore be trapped for long times in a metastable orientation. The slow (temperature-dependent) relaxation from this metastability is responsible for the hysteresis and the other effects discussed below.

Fig. 3(a) also indicates that as temperature is lowered, new steps arise out of the saturation curve while others that were clearly observable at higher temperatures become less pronounced. These "frozen" steps can be recovered when the magnetic field is swept more slowly, emphasizing the fact that the steps are related to a relaxation phenomenon. In fact, if one stops sweeping the loop at any point, the magnetization will relax toward its equilibrium value whether or not the field is tuned to one of the steps, as will be discussed below.

In Fig. 3(b) the slope dM/dH of the curves shown in Fig. 3(a) is shown as a function of external magnetic field. Maxima (corresponding to the steepest portion of the steps) are found at particular values of the field that appear to be independent of temperature. A careful analysis shows that the "step field" – the value of external field H for each step – does shift slightly with temperature. While one might conjecture that this slight dependence is intrinsic, it is also found that the position of each step similarly depends on the rate at which the magnetic field is swept. The common thread that links both cases is that the step field has a slight linear dependence on the instantaneous value of the magnetization at which the step occurs [7]. This dependence can be easily explained by noting that each individual Mn_{12} molecule sees not only the applied field, but also the mean dipolar field from all of its neighbors. It is tempting to equate this effective field, H_{eff}, with the magnetic induction, $B = H + 4\pi M$, as has been done in some reports [6, 7, 63, 64] (including some by this author). However, it was pointed out by Sessoli [71] that this relation, despite its intuitive appeal, is too simplistic and predicts a stronger dependence of H_{eff} on M than is observed. A more careful calculation [72] of the classical dipole field on Mn_{12} molecule due to its neighbors (treating each molecule as a point dipole and extending the number of neighbors until the results converge) yields very good agreement with data: $H_{eff} \approx H + 7.1M$.

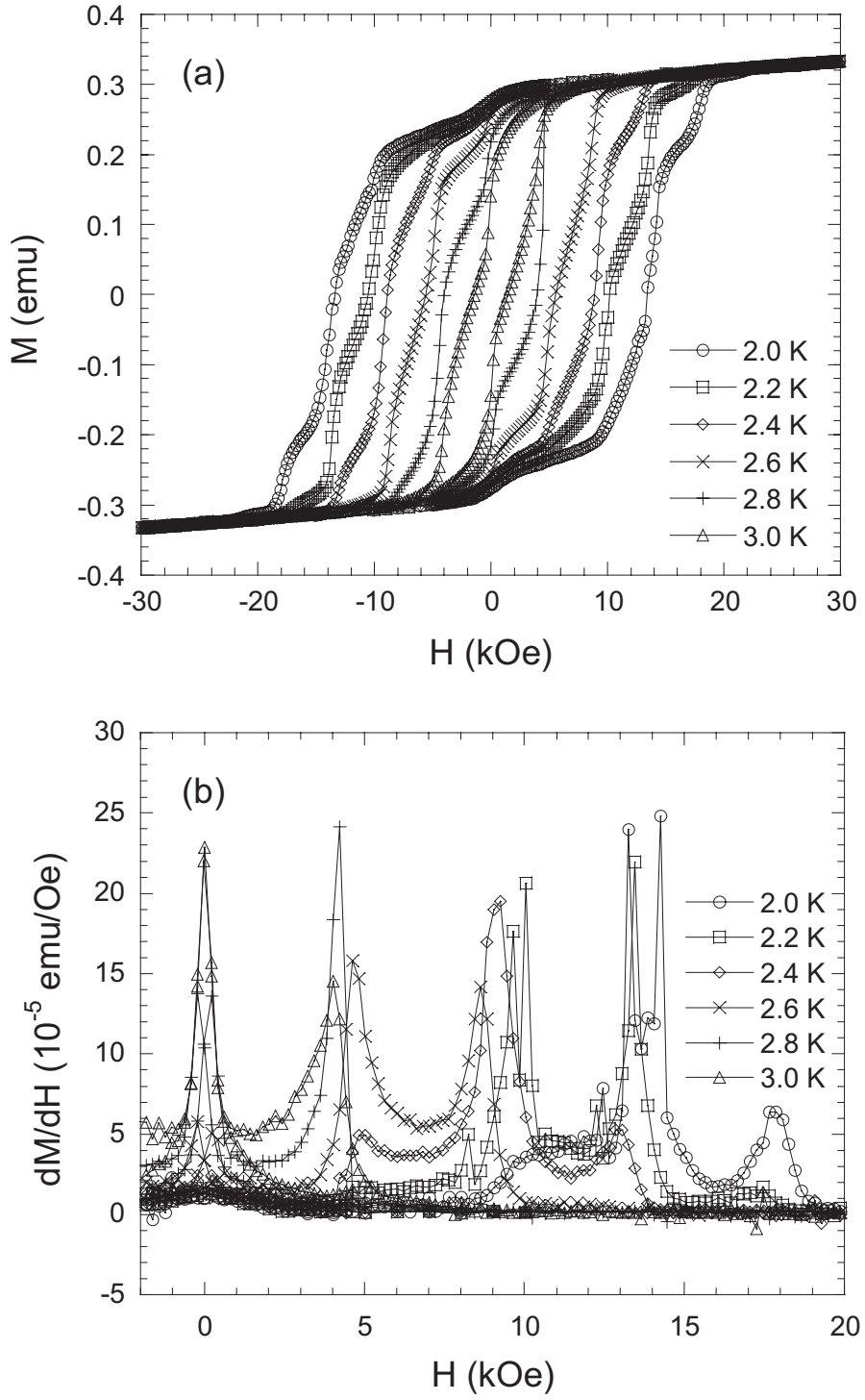

Figure 3 (a) Hysteresis loops of a powdered sample of Mn_{12} that has been oriented in a paraffin matrix. At all temperatures shown steps are observed in the hysteresis loops as the field is increased (in either direction) from zero but not when it is decreased. (b) Derivative of the hysteresis loops in (a). The peaks indicate the fields at which the steps in the loops are steepest. The data indicate that the steps always occur near the same values of magnetic field.

Fig. 4 shows the value of H_{eff} at which a step occurs as a function of step number *n*, where the steps have been labeled by integers starting with the one at zero field labeled #0. The straight-line fit (solid line) indicates that there are steps at equal intervals of approximately 4.5 kOe. The figure shows seven steps, including #0, have been observed. A total of 12 steps have been seen in pulsed-field measurements [73] at 1.53 K and in measurements at temperatures below 1 K [66]. One can estimate empirically the total number of steps expected from the data in the hysteresis loops by noting the temperature at which a step first appears. This temperature, T^*, should characterize the barrier height *U*, which decreases with applied field as $(H - H_c)^2 \sim (n - n_c)^2$, since the step number *n* is proportional to *H* (Fig. 4). This implies that $n - n_c \sim T^{*1/2}$. Fig. 5 shows the step number plotted as a function of this characteristic temperature $T^{*1/2}$. The linear fit extrapolates to $n_c = 20.6$ at zero temperature, indicating that there could be about 21-22 steps (counting n = 0), which is consistent with the prediction that the number of steps should be 20 (see below). The fact that a total of only 12 steps have been observed when one includes data down to the lowest temperatures is most likely because the barrier gets so low for the higher-numbered steps that the ground-state tunneling rate becomes too fast to measure.

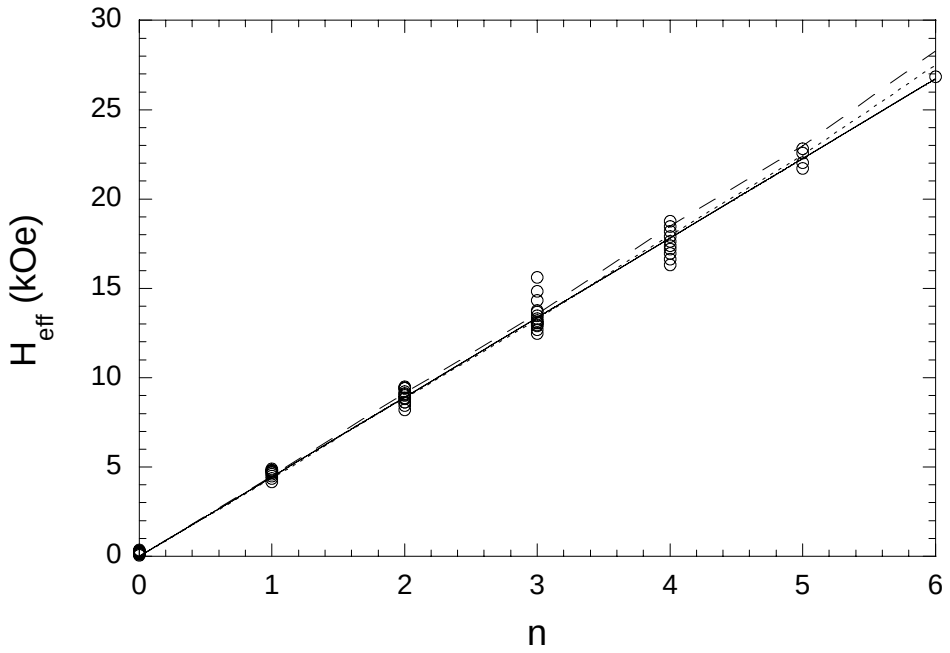

Figure 4 The field H_{eff} at which a step occurs as a function of step number. The steps are labeled by integers starting with the one at zero field (step #0). The linear (solid line) fit indicates that a step occurs about every 4.5(1) kOe. The dotted (dashed) line indicates the expected values of H_{eff}, assuming that tunneling always occurs between levels that are $m_b = 3\,(4)$ below the top of the barrier.

For a zero-field-cooled sample, Fig. 6 shows the magnetization measured in various magnetic fields as the temperature is increased. For a given field, the magnetization increases with temperature as the additional thermal energy allows more spins to overcome the anisotropy barrier and line up with the applied field. The magnetization peaks at the blocking temperature T_B where the spins reach thermal equilibrium; the subsequent decrease in magnetization is due to the Curie-law-like competition between magnetic and thermal energies. T_B shows an overall decrease as the field is raised, as expected for superparamagnetic particles in which the anisotropy barrier is reduced by the applied field. However, the curve obtained at 9.0 kOe exhibits an abrupt shift toward lower temperatures. Similar shifts are found at each of the fields where steps are seen in the hysteresis loops. In Fig. 7 the blocking temperature is plotted as a function of measuring field from 100 Oe to 19 kOe. Superimposed on an overall decrease as a function of field, the blocking temperature T_B exhibits periodic dips at the same values of field as the steps in the hysteresis loops. Ignoring the dips, one obtains a zero-field blocking temperature of ~3.5 K. Using a measurement time of 100 seconds (the time between data points) and an Arrhenius prefactor, τ_0, of 2 x 10^{-7} seconds [36, 46-49, 59, 60], one can estimate the size of the energy barrier to be $U = kT_B \ln(t_{meas} / \tau_0) \approx 71K$, in fair agreement with published results [36, 46-49, 54, 55, 59, 60, 62, 63]. The periodic steps in the hysteresis loop, accompanied by dips in the blocking temperature at the same magnetic fields imply that the relaxation rate is significantly faster whenever the magnetic field is an integer multiple of 4.5 kOe.

This can be confirmed directly by looking at the magnetic relaxation of the system. For a sample cooled to 2.4 K in zero field and measured in a field of 9.0 kOe or 9.5 kOe, Fig. 8 shows the difference between the magnetization and its asymptotic value, M_0, plotted as a function of time on a semilogarithmic scale. Note that the long-time tail of the curve appears to be close to exponential, but that the earlier data (most of the decay of the moment) is faster. There are several possible explanations for this, including the existence of a second species of Mn_{12} with a smaller barrier and, hence, faster relaxation rate as well as the fact that the mean dipolar field in the sample is changing as the sample relaxes. Both of these effects will be discussed a bit later in this chapter. Nevertheless, independent of the exact form of the relaxation, there is dramatically faster relaxation at 9.0 kOe than at 9.5 kOe. Disregarding the faster-than-exponential decay during the initial ~2000 seconds, fits to an exponential form $M = M_0(1-e^{-(t-t_0)/\tau})$ with M_0, t_0 and τ as free parameters yield time constants of 1048 s and 2072 s for 9.0 kOe and 9.5 kOe, respectively.

Repeating this procedure at various fields and temperatures one obtains the relaxation rate data shown in Fig. 9. Here the rate $\Gamma = 1/\tau$ is plotted as a function of external field H at two temperatures. One can identify four maxima in the decay rate: at approximately $H = 4.5\ n$ kOe, with $n = 0$, 1, 2, and 3.

All of the above results can be explained through a simple model of thermally assisted resonant tunneling using the Hamiltonian Eq. (2). If the field is applied along the easy (z) axis, and one ignores $\mathcal{H}'$, the eigenstates of Eq. (2) are $|m\rangle$, the eigenstates of S_z. The system can then be represented schematically as a double-well potential, as shown in Fig. 1, where the $2S + 1 = 21$ energy levels correspond to different projections of the spin along the easy axis. An applied field is responsible for the asymmetry in the figure, making one well, say spin up, lower in energy than the other. In zero applied field, the wells are symmetric and there is a two-fold degeneracy for each state (except $m = 0$): $m = 10$ and -10, $m = 9$ and -9, etc. When the field is raised, levels in

one well will move up while levels in the other well will move down and for certain values of field levels in opposite wells will again come into resonance.

The model of thermally assisted resonant tunneling is as follows. When the field is such that no pairs of levels are near resonance, the system must relax by thermal activation over the entire potential barrier. However, if two levels near the top of the barrier (where the tunneling rate is large) come into resonance, the system no longer needs to be activated to the top of the barrier but only to the resonant pair, where it can tunnel through the barrier quickly. Thus, tunneling effectively cuts off the top of the barrier, increasing the interwell relaxation rate and thus giving rise to the steps in the hysteresis loops and the dips in the blocking temperature.

It is straightforward to calculate the fields at which levels m and m' (in opposite wells) come into resonance. The results is:

$$H_{m,m'} = \frac{Dn}{g_z \mu_B}\left[1 + \frac{A}{D}(m^2 + m'^2)\right] \tag{3}$$

where g_z is the Landé g factor and $n = m + m'$ can be identified with the step index above. If one ignores the second term in the brackets, the resonant field is an integer multiple of $D/g\mu_B$. This is consistent with Fig. 4, which shows steps at regular intervals of field. From the fact that the steps occur approximately every 4.5 kOe, one can deduce that D/g = 0.210 cm^{-1}, which is about 5% larger than one would expect from the best spectroscopic determinations of D and g. The above analysis was the approach taken in the early reports [4-6, 64, 65] before the discovery [10, 11, 74] of the fourth-order anisotropy term in Eq. (2). The full Eq. (3) (including the second term in the brackets) shows that the resonance fields are no longer simply proportional to n and, therefore, one may not immediately expect the observed linear dependence. This apparent inconsistency can be resolved by assuming that for every n, the tunneling always occurs between states that are a fixed number of levels m_b below the top of the barrier (i.e., in Fig. 1 m_b = 3). Then, using the most accurate measured values for the Hamiltonian parameters D = 0.3855 cm^{-1} and A = 7.8 x 10^{-4} cm^{-1} [14] and g_z = 1.94 [10], for a given value of m_b one can determine without any adjustable parameters the expected resonance fields. The results for m_b = 3 (4) are shown by the dotted (dashed) line in Fig. 4. The agreement with the data is quite satisfactory for both values although somewhat better for m_b = 3.

Another satisfactory aspect of this model is the number of resonances it predicts. Since there are $2m + 1 = 21$ levels, there can be as many as 20 level crossings before the field reduces the barrier to zero. In this light, the result of $n_c \approx 21$ deduced from Fig. 5 using data up to $n = 6$ is a fortuitously good result. If one further constrains, as above, that tunneling always occurs from, say, m_b = 3 (4), then there can be no more than 16 (14) resonances before the ground state in the metastable well becomes the tunneling level. Given the roughness of the constant-m_b approximation, this number is not inconsistent with the observed 12 resonances.

All of the data shown above shows a strong temperature dependence: the hysteresis-loop width increases with decreasing temperature and the measured relaxation rate varies exponentially with temperature. This implies that the relaxation mechanism is thermally assisted and cannot be accounted for simply in terms of tunneling out of the ground state. Estimates of the

tunneling rate from the ground state under the relevant experimental conditions yield rates that are orders of magnitude slower than the observed relaxation rate (see Table I).

Table I: Tunneling splitttings for the $n = 0$ ($m' = -m$) resonance for different m values calculated using Eq. (6) with S = 10, $B_x = 0.1$ kG and D = 0.41 cm^{-1}.

m	$\Delta_{m,-m}$ (Hz)
1	3.2×10^{8}
2	1.1×10^{5}
3	3.5×10^{0}
4	2.3×10^{-5}
5	4.7×10^{-11}
6	3.7×10^{-17}
7	1.2×10^{-23}
8	1.7×10^{-30}
9	1.1×10^{-37}
10	2.11×10^{-45}

Further confirmation for the picture of field-tuned, thermally assisted resonant tunneling out of a metastable spin state has been provided by AC susceptibility measurements [62, 63]. In these studies, it was found that the relaxation rate obeyed an Arrhenius law and that the inferred barrier height varied with applied magnetic field by as much as 12 K. This implies, first, that the picture that tunneling effectively reduces the energy barrier for thermal activation is correct and, second, that the tunneling is occurring 3 or 4 levels below the top of the barrier, consistent with the discussion above. Evidence for resonant tunneling also appears in the magnetic-field dependence of specific heat [62, 67-69] and NMR [70] data.

In sum, then, the proposed model explains all of the experimental observations: (1) Resonant tunneling causes the transition rate to increase at values of the magnetic field that yield energy-level crossings in the two wells. (2) When the field is reduced from saturation, no steps are seen in the hysteresis loops because the spins are already in the lower-energy potential well. When the field is reduced to near zero or reversed, the populated well becomes metastable allowing resonant transitions out of the populated states and the corresponding steps. (3) The higher-numbered steps have progressively faster magnetic relaxation times because the anisotropy barrier is lowered by the applied field. Therefore, lower temperatures are needed to observe them. (4) The fields at which the steps occur (roughly regular intervals of field) can be quantitatively explained using the Hamiltonian Eq. (2) and the assumption that tunneling is occurring from a level $m_b = 3$ or 4, i.e. 3 or 4 levels below the top of the barrier.

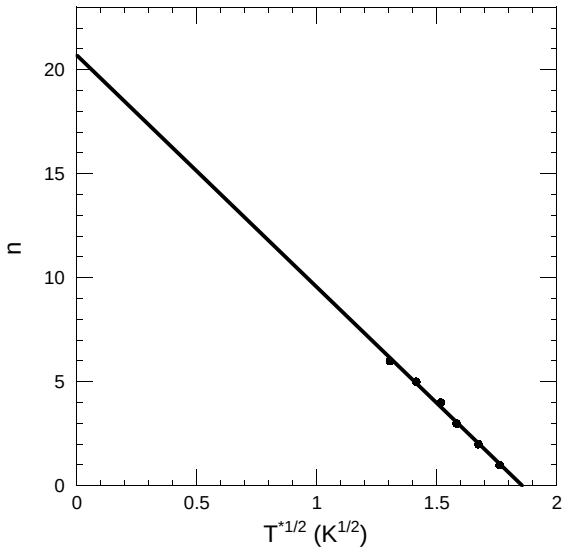

Figure 5 Step number n as a function of $T^{*1/2}$. The straight-line fit indicates that there may be as many as 21-22 steps, including $n = 0$, consistent with the fact that there can be no more than $2S = 20$ level crossings.

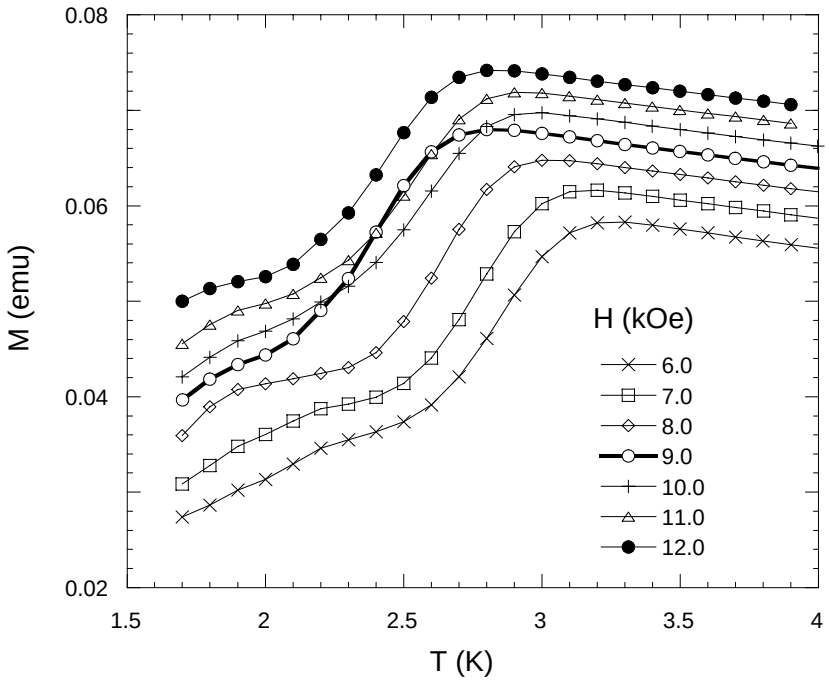

Figure 6 Zero-field-cooled curves for Mn_{12} at various magnetic fields, as indicated. The magnetization is plotted as a function of increasing temperature for a sample of oriented powder in a Stycast matrix. The curve taken at 9.0 kOe is anomalous, apparently shifted toward lower temperatures relative to neighboring curves.

III. "WHAT CAUSES TUNNELING?"

In this section, I will show that, despite the clarity of the above explanation, there are still some open questions regarding the mechanism of tunneling and relaxation in Mn_{12}. (The situation is somewhat clearer in another molecular magnet, Fe_8, where much of $\mathcal{H}'$, the off-diagonal part of the Hamiltonian, has been determined with fair accuracy by spectroscopic means [75, 76].) I will show that Mn_{12} violates a selection rule and thereby that tunneling must, at least in part, be driven by some transverse magnetic field, presumably of hyperfine origin, and describe some of the work to elucidate the precise nature of this field. Another mechanism, a transverse tetragonal anisotropy, has been discussed in the literature as a possible additional source of tunneling. However, the experimental evidence for its existence is ambiguous.

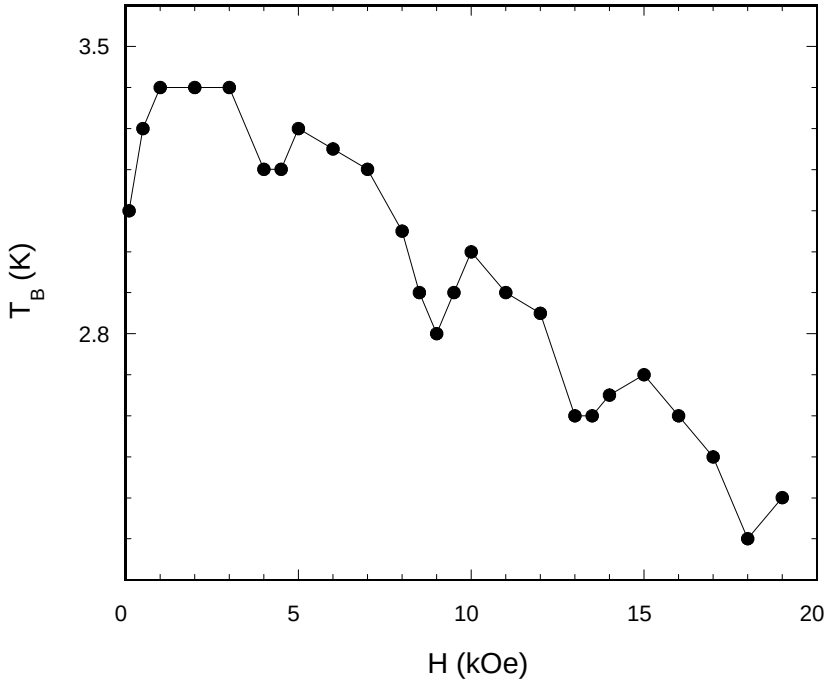

Figure 7 Blocking temperature as a function of field. The blocking temperature was taken from the peaks of the curves in Fig. 6 and similar curves at other fields. The dips in the blocking temperature occur at the same fields as the steps in the hysteresis loops.

III.A. Selection-rule Violation

In theoretical discussions, magnetic tunneling is often attributed to the presence of a transverse component in the magnetocrystalline anisotropy tensor [29-32]. Since the anisotropy arises from spin-orbit coupling and is therefore even under time reversal, it must appear as an even power of the spin operator **S**. Mn_{12} has tetragonal symmetry, so that the lowest-order transverse term is

$$\mathcal{H}'_{anis} = \frac{C}{2}(S_+^4 + S_-^4) \tag{4}$$

where S_+ and S_- are the usual spin raising and lowering operators. This form only allows transitions that obey the selection rule $\Delta m = \pm 4q$ (integer q). This would, in turn, prohibit every other step: for whenever the system is tuned to an odd-numbered step (e.g. $n = 1$), the levels in resonance are always matched even/odd and odd/even (e.g. 10/-9, 9/ -8, 8/-7,...), yielding a forbidden, odd Δm for all matched levels. This transverse-anisotropy selection rule can be thought of as a generalization of Kramers' theorem that, in the absence of a magnetic field, half-integer spin systems cannot tunnel (have at least two-fold degeneracies): for integer spins only the even-numbered resonances are allowed, while for half-integer spins, only the odd-numbered resonances are allowed.

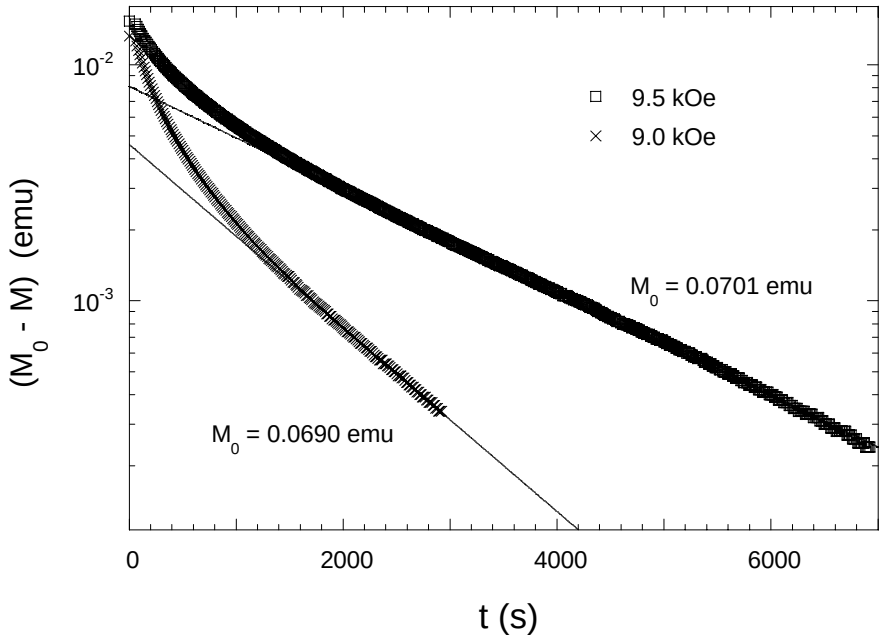

Figure 8 Relaxation curves on and off resonance. The difference between the magnetic moment and its asymptotic value is plotted on a logarithmic scale as a function of time for a sample of oriented powder in a Stycast matrix. The sample was cooled in zero field to 2.4 K and then the indicated field was applied. The data show that the relaxation is markedly faster for the curve taken with a field of 9.0 kOe, which is near where one of the steps occurs in the hysteresis loops. The straight-line fits are to exponentials using data for t > 2000 s.

The data shown in the previous section indicate that all steps are observed, even the "forbidden" ones. In fact, for Mn_{12} there is no hint of an asymmetry between the allowed even steps and the forbidden odd steps. A source of tunneling that does not prohibit any steps is a small transverse magnetic field B_x, which gives rise to a term of the form

$$\mathcal{H}'_B = g_x \mu_B B_x S_x = \frac{g_x \mu_B B_x}{2}(S_+ + S_-) \tag{5}$$

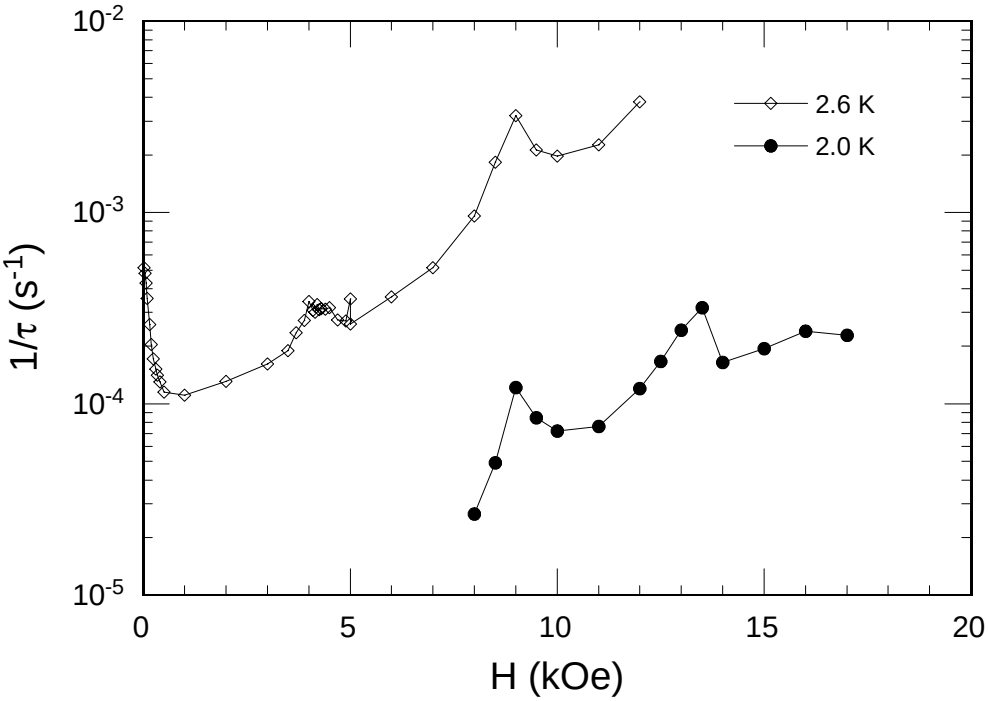

Figure 9 Relaxation rate as a function of field for a powdered sample in a paraffin matrix. The rate was determined from fits to relaxation curves similar to those in Fig. 8. The peaks in the relaxation rate occur at the same fields as the steps in the hysteresis loops.

This allows all transitions $\Delta m = \pm 1q$, prohibiting no steps. Such a transverse field can arise in three possible ways: it can be applied externally, it can come from dipolar interactions between neighboring molecules or it can come from the hyperfine interaction with the Mn (and other) nuclei in the system. In the experimental data shown above, no external transverse field was intentionally applied. One may conjecture [77, 78] that (especially in the oriented-powder samples) the sample's easy axis is not perfectly aligned with the applied field, giving rise to a small transverse component of the field. This argument cannot apply to the zero-field resonance, of course, since the applied field is near zero. However, for the usual Mn_{12} molecule with integer spin 10 the zero-field resonance is allowed by the transverse-anisotropy selection rule, as discussed above. Some variants of Mn_{12}, in which the magnetic core is chemically reduced, have a half-integer spin of 19/2 [79, 80]. These (as well as an unrelated molecule called Mn_4 with spin 9/2 [81]) also show a clear zero-field resonance, which does in fact violate the transverse-anisotropy selection rule and Kramers' theorem. This rules out the possibility that the tunneling is due to a misaligned magnetic field.

Dipole fields as a possible cause of tunneling have been discounted by a study in which the Mn_{12} molecules were dispersed in a glassy matrix in which dipole interactions among molecules were negligible [82]. At least for the zero-field resonance that could be studied in that sample, the

relaxation rate as a function of field behaved largely the same as for a crystalline sample.* Therefore, hyperfine fields seem to be the most likely source of the transverse field.

III.B Transverse-Field Experiments

Before discussing the experiments that probed the role of hyperfine fields, I will digress a bit to show how an intentionally applied transverse field can be used to test the model of thermally assisted resonant tunneling.

Fig. 10(a) shows the magnetization as a function of longitudinal field for various fixed values of transverse field at 2.0 K [83]. For each value of transverse field, one quarter of the hysteresis loop is shown, the other quarters being either redundant or featureless. In taking this data, a sample rotator was used to adjust the angle between the sample's easy axis and the direction of the applied magnetic field. This angle was varied as the field was swept such that the transverse component of the field remained constant. It is immediately clear that, while the height of each step varies with transverse field, the steps always occur at the same values of longitudinal field, independently of the value of the transverse field. This is clearly demonstrated by the derivative of the magnetization, shown in Fig. 10(b). Similar conclusions were drawn by Hernandez et al. [6] and Lionti et al. [84]. This result is consistent with calculations that show that the resonance condition Eq. (3) (in the simple case of A = 0) is invariant in the presence of a transverse field to at least fourth order in perturbation theory [85, 86].

To leading order in perturbation theory, the tunnel splitting between resonant levels m and m' depends on the transverse field B_x as

$$\Delta_{m,m'} = \frac{2D}{[(m-m'-1)!]^2}\sqrt{\frac{(s+m)!\ (s-m')!}{(s-m)!\ (s+m')!}}\left(\frac{g\mu_B|B_x|}{2D}\right)^{m-m'}, \qquad (6)$$

again in the simple case A = 0 [86, 87]. This formula is an extension of one for ground-state tunneling originally derived by Korenblit and Shender [88]. The unsurprising upshot of this result is that tunneling between levels near the top of the barrier is faster. A quantitative tabulation of Eq. (6) for the $n = 0$ resonance for a transverse field of 0.1 kG is given in Table I. It is clear that the tunnel splitting increases by several orders of magnitude each time one climbs up one resonant pair towards the top of the barrier (see Fig. 1). This lends credence to the picture that tunneling is occurring primarily in one pair of resonant levels. As one turns up the transverse field, the tunnel splitting for each pair should increase and, therefore, the relevant tunneling pair should drop from, say, $m_b = 3$ to $m_b = 4$. Consequently, the relaxation rate should increase in a series of jumps and plateaus [7, 87].

A detailed study of the relaxation rate as a function of both longitudinal and transverse field components was performed on a single crystal [83]. In Fig. 11, the measured on-resonance and off-resonance relaxation rate (extracted from the long-time tail of the relaxation curves, as above) is plotted on a semilogarithmic scale as a function of transverse field for the $n = 1$ resonance at T

* One might object that the zero-field resonance is not a forbidden resonance and so no transverse field is necessary for it. While this possibility has not been experimentally ruled out (i.e. by a similar study of a half-integer variant of Mn_{12}), it seems unlikely given that all of the resonances have about the same magnitude.

= 2.7 K. One sees that both on and off resonance, the relaxation rate seems to have a plateau between 2 and 3 kOe. A similar plateau was seen in data taken at 2.6 K. There has yet to be a more thorough study of the transverse-field dependence of the relaxation rate to confirm the expected series of jumps and plateaus.

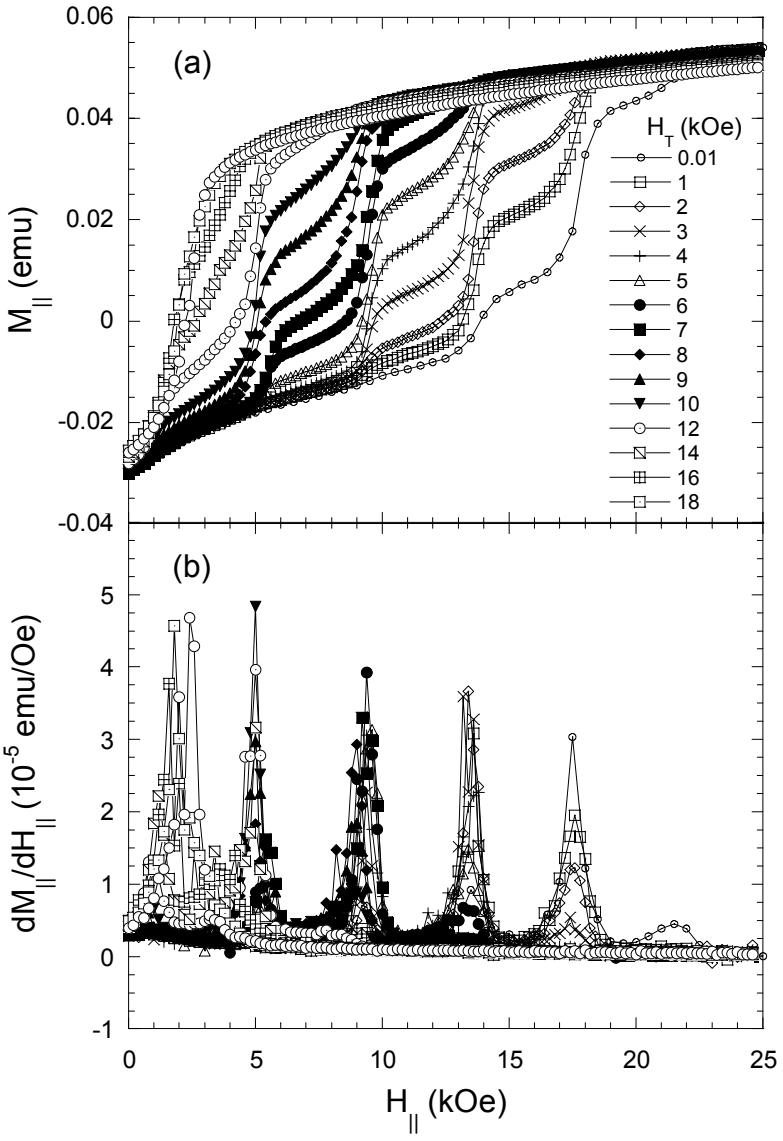

Figure 10 Magnetization steps for various transverse fields. (a) Magnetization as a function of longitudinal field for several values of transverse field at 2.0 K. (b) The derivative of the curves in (a). The steps occur at the same values of longitudinal field for all values of transverse field. A small misalignment of the sample rotator is responsible for the fact that the $n = 0$ step is not at zero field.

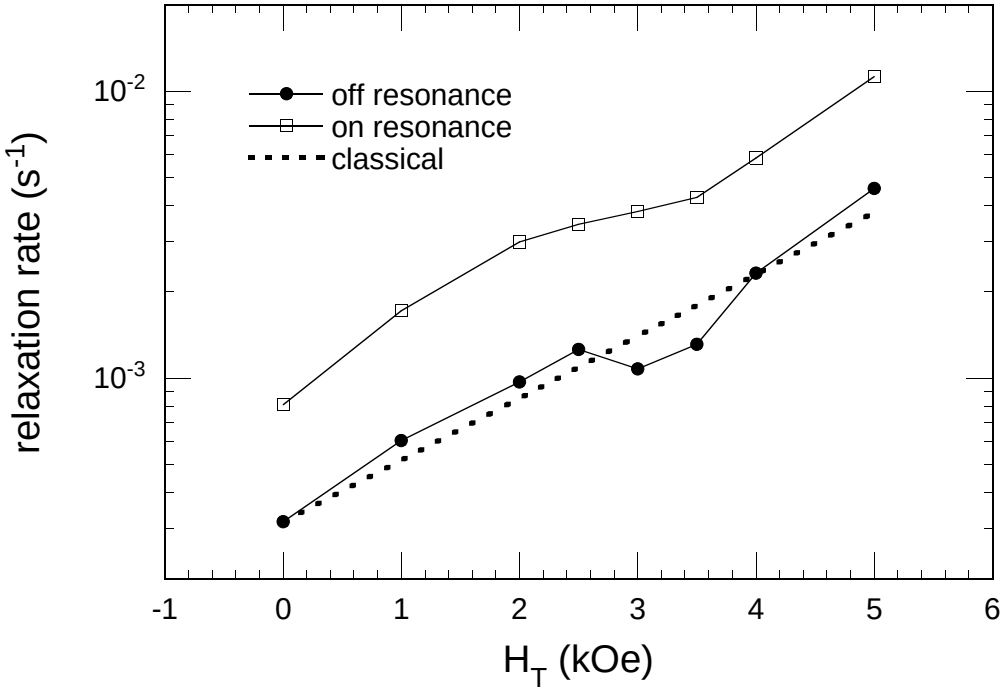

Figure 11 Relaxation rate on and off resonance as a function of transverse field. The straight line in this figure is the expected classical rate discussed in the text.

One interesting complication in interpreting the results of Fig. 11 in terms of tunneling is the fact that a transverse field also has the well-known effect of lowering the spin's classical energy barrier. The expected classical dependence of the relaxation rate is shown by the straight line (labeled "classical") in the figure, where the slope was calculated with no free parameters and the vertical intercept was simply fixed to correspond to the measured off-resonance rate at $H_x = 0$. The fact that the general trend of the data seems to follow this line is more than simply a coincidence. In the limit of a large (classical) spin there is a rigorous quantum-classical correspondence between the top of the classical energy barrier and the resonant pair for which the tunnel splitting is comparable to the anisotropy parameter D [86]. Thus, while it is tempting (and true!) to attribute the general increase in the relaxation rate as a function of transverse field to tunneling, the result nevertheless also simply confirms that a transverse field reduces the classical energy barrier. The only non-classical effect here is the observed plateau.

III.C. Details of the relaxation process

Let us return to the issue of the relaxation in Mn_{12} when the tunneling is not augmented by an external transverse field. We established earlier in this section that the most likely mechanism of tunneling is a transverse field due to hyperfine fields. Some early theoretical estimates [89] yielded an effective Mn hyperfine field of as high as 300 – 500 Oe. This led to the search [90] for evidence of random hyperfine fields in the line shape of the tunneling resonances. For it was expected that the hyperfine fields would give rise to inhomogeneous (Gaussian) broadening of the

resonance. Results for an oriented-powder sample in a paraffin matrix are presented in Fig. 12, where the relaxation rate is plotted as a function of field for four different temperatures. The data for each temperature fit very well to a Lorentzian function. This indicates that any inhomogeneous broadening of the resonance is negligible. Thus, no evidence of hyperfine fields could be found in the data. From the fits the full width is found to be 267, 236, 270 and 271 Oe for 2.5, 2.6, 2.7 and 2.8 K, respectively. This is consistent with the width found by fitting AC susceptibility data to a Lorentzian [63].

The Lorentzian shape of the tunneling resonance suggests that it represents some dynamical aspect of the relaxation process. One interpretation is that the data reflect the natural line shape of the levels that are involved in the tunneling, the width then being a measure of the levels' lifetimes. If we assume that the tunneling is occurring between, say, levels $m = 3$ and $m = -3$, then the observed width of ~250 Oe corresponds to a lifetime $h / g\mu_B(2m)\Delta H$ of 2.5 x 10^{-10} s. While this is typical of spin-lattice relaxation times in many magnetic systems, the measured Arrhenius prefactor $\tau_0 \left(=2\pi/\omega_0\right)$ for Mn_{12} is around 10^{-7} s and it is this number that is expected [56] to characterize the typical lifetime of excited states in the system. Another interpretation is that the line width represents the tunnel splitting itself. However, the tunnel splitting should be a sensitive function of transverse field (Eq. (6)), but the line width does not show any strong dependence on transverse field [83].

Understanding the details of the thermally assisted tunneling process has been a challenging theoretical problem. While no completely satisfying explanation exists for the experimental data, some important issues have become clearer. There have been numerous theories of ground-state (i.e. not thermally assisted) tunneling in the molecular magnets [91-95], which are not relevant to the current discussion, although some will be considered a bit later in this chapter. In the discussion that follows I borrow several ideas from various theories of thermally assisted resonant tunneling [7, 56, 77, 78, 87, 96-99]. While there are several important details that make each of these theories distinct, I will initially concentrate on the aspects that most have in common and then discuss their differences.

Most of the theories use some version of a master-equation approach, which can be summarized as follows. Each spin eigenstate $|m\rangle$ has a probability p_m of being occupied (i.e. each p_m is a diagonal element of the density matrix in the $|m\rangle$ representation). Transitions between $|m\rangle$ states can occur in one of two ways: by the absorption or emission of phonons or by tunneling. Phonon-induced processes are governed by a spin-phonon interaction Hamiltonian of the form:

$$\begin{aligned}\mathcal{H}_{sp} &= g_1(\varepsilon_{xx}-\varepsilon_{yy})(S_x^2-S_y^2)+g_2\varepsilon_{xy}\left\{S_x,S_y\right\}+\\ &+g_3(\varepsilon_{xz}\left\{S_x,S_z\right\}+\varepsilon_{yz}\left\{S_y,S_z\right\})+g_4(\omega_{xz}\left\{S_x,S_z\right\}+\omega_{yz}\left\{S_y,S_z\right\}),\end{aligned} \tag{7}$$

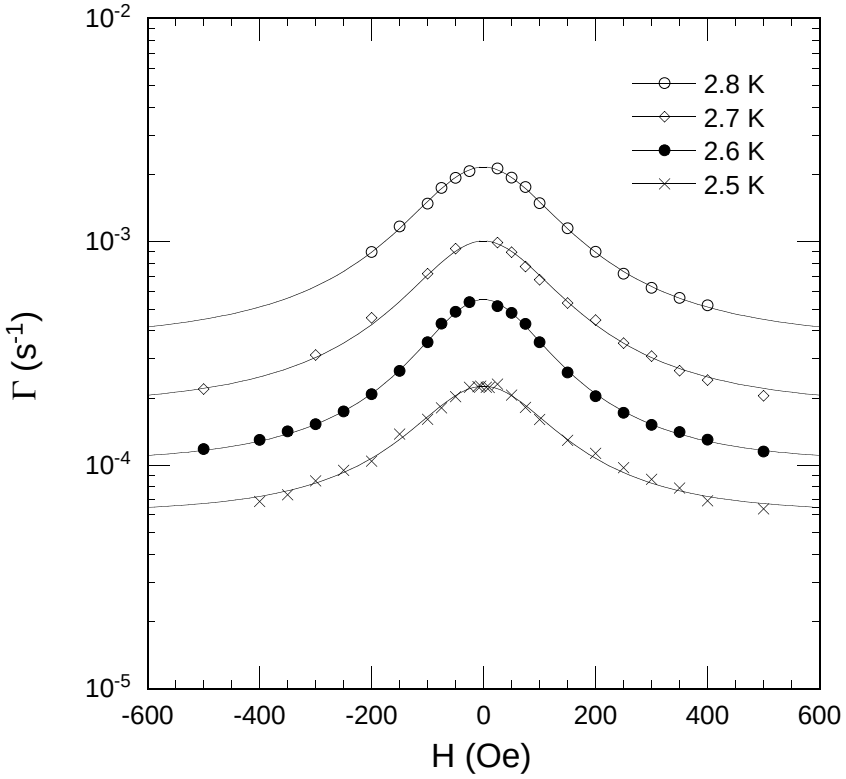

Figure 12 Line shape of resonance $n = 0$. The relaxation rate is plotted on a logarithmic scale as a function of field near zero field for a sample of oriented powder in a paraffin matrix. The data have been fit to Lorentzian functions plus a uniform background.

where $\varepsilon_{\alpha\beta}(\omega_{\alpha\beta}) \equiv \frac{1}{2}\left(\partial_\alpha u_\beta + (-)\partial_\beta u_\alpha\right)$ is the strain (rotation) tensor with **u** the displacement vector, the curly brackets indicate anticommutation and the g_i are coupling constants. It is important to note that the first two terms of Eq. (7) implicitly contain the spin raising and lowering operators, S_+ and S_-, to second order. This allows a single phonon to change the spin quantum number *m* by 2: $|m\rangle \rightarrow |m \pm 2\rangle$. The other terms, which are linear in S_+ and S_-, allow "first-order" transitions: $|m\rangle \rightarrow |m \pm 1\rangle$. Transition rates for both of these kinds of processes are given by golden-rule-type expressions:

$$\gamma_{m\pm1,m} \propto \frac{E_{m\pm1,m}^3}{\rho c^5 \hbar^4} \frac{\left|\langle m \pm 1 | \mathcal{H}'_{sp} | m \rangle\right|^2}{e^{\beta E_{m\pm1,m}} - 1}$$
$$\gamma_{m\pm2,m} \propto \frac{E_{m\pm2,m}^3}{\rho c^5 \hbar^4} \frac{\left|\langle m \pm 2 | \mathcal{H}'_{sp} | m \rangle\right|^2}{e^{\beta E_{m\pm2,m}} - 1}, \tag{8}$$

where $\mathcal{H}'_{sp}$ is the spin-operator part of $\mathcal{H}_{sp}$, $E_{m,m'}$ is the difference in energy between $|m\rangle$ and $|m'\rangle$, ρ is mass density, *c* is the speed of sound and the constants of proportionality depend on

the relative strengths of the coupling constants g_i in Eq. (7). Incoherent tunneling between levels $|m\rangle$ and $|m'\rangle$ in opposite wells can be described by a Lorentzian function:

$$\Gamma_{m,m'} = \frac{\gamma \Delta_{m,m'}^2}{E_{m,m'}^2 + \gamma^2/4 + \Delta_{m,m'}^2}, \tag{9}$$

where $\Delta_{m,m'}$ is the bare tunnel splitting in the absence of dissipation (given by, e.g., Eq. (6) if tunneling is induced entirely be a transverse magnetic field). The resonance width γ is the concatenated level widths of $|m\rangle$ and $|m'\rangle$; i.e. $\gamma \approx \gamma_m + \gamma_{m'}$ with γ_m being the total inverse lifetime of $|m\rangle$, which can be calculated with the help of Eqs. (8). Eq. (9) is valid as long as $\Delta_{m.m'} << \gamma$ or $E_{m.m'} >> \Delta_{m,m'}$, the incoherent regime. In the opposite limit in which tunneling is coherent, the analysis becomes complicated by the need to carefully treat the off-diagonal elements of the density matrix. For the purposes of simplicity I will limit discussion to the incoherent tunneling case.

For a given set of spin-phonon transition rates, Eqs. (8), and tunneling rates, Eq. (9), the population of the state $|m\rangle$ will obey

$$\begin{aligned} \dot{p}_m = \Gamma_{m,m'}(p_{m'} - p_m) - (\gamma_{m,m+1} + \gamma_{m,m+2} + \gamma_{m,m-1} + \gamma_{m,m-2})p_m + \\ + \gamma_{m+1,m}p_{m+1} + \gamma_{m+2,m}p_{m+2} + \gamma_{m-1,m}p_{m-1} + \gamma_{m-2,m}p_{m-2}. \end{aligned} \tag{10}$$

With 21 of these equations for a spin-10 system like Mn_{12}, a formal solution, while straightforward, is practically unwieldy. Numerical solutions are also straightforward, but do not necessarily elucidate the essential physics. However, one can make some reasonable arguments to get at the crux of the relaxation process.

For simplicity, let us limit our discussion to only "first-order" spin-phonon transitions. Consider states on the $m > 0$ side of the barrier, where states with higher *m* values lie lower. Thus, for example, $\gamma_{m,m-1}$ corresponds to an "up" transition and $\gamma_{m,m+1}$ to a down transition, as illustrated schematically in Fig. 13. Now, as Table I demonstrates, the tunneling rate varies by several orders of magnitude each time one climbs up the ladder of states. Except at the lowest temperatures, some of the lower levels will have tunneling rates much slower than the rate for phonon absorption: $\Gamma_{m.m'} << \gamma_{m.m'-1}$. These low-lying levels will rapidly achieve a sort of local thermal population within the well much faster than the well is depleted. Thus, $p_m = e^{-\beta E_{m,S}} p_S$ for these levels. Let us consider the highest level $|m\rangle$ for which this is true. The tunneling rate for the next highest level $|m-1\rangle$ is sufficiently large such that its population is transferred into the opposite well faster than the level can be thermally repopulated. The population in $|m\rangle$ can be transmitted to the opposite well in one of two ways. The first is direct tunneling to the level $|m'\rangle$ in the right well with which it is resonant. The total rate for this process is $\Gamma_{m,m'} e^{-\beta E_{m,S}}$

(tunneling rate times population of the level). The other process involves activation to $|m-1\rangle$ and yields a total rate of $\gamma_{m,m-1}e^{-\beta E_{m,S}} = (\gamma_{m-1,m}e^{-\beta E_{m-1,m}})e^{-\beta E_{m,S}} = \gamma_{m-1,m}e^{-\beta E_{m-1,S}}$. The tunneling rate for level $|m-1\rangle$ does not come into play here since, by construction, it is faster than the thermal repopulation rate and the latter is therefore the rate-limiting step.

Which of the two processes, tunneling from $|m\rangle$ or activation to $|m-1\rangle$, dominates the relaxation depends sensitively on temperature, since their ratio is

$$r_m = (\Gamma_{m,m'} / \gamma_{m-1,m})e^{\beta E_{m-1,m}} . \tag{11}$$

As one raises the temperature, for a given $|m\rangle$, r_m rapidly changes from $r_m >> 1$ to $r_m << 1$ and the dominant level shifts from $|m\rangle$ to $|m-1\rangle$. By analogy, at some higher temperature, it will again shift, this time from $|m-1\rangle$ to $|m-2\rangle$, etc. This climbing up the ladder of levels will not continue all the way to the top of the barrier, however, because for some level $|m_{top}\rangle$ the tunneling rate $\Gamma_{m_{top},m'_{top}}$ will be larger than the phonon-emission rate $\gamma_{m_{top}-1,m_{top}}$ and, hence, $r_m > 1$ at all temperatures. This level is then the effective top of the barrier and at high temperatures tunneling will always occur from this level. This explains the observed Arrhenius law at high temperatures when the field is tuned to a resonance [62, 63]: resonant tunneling has reduced the barrier height to $E_{m_{top}} - E_S$ and it is this energy, not the full barrier height *U*, that goes into the Arrhenius law.

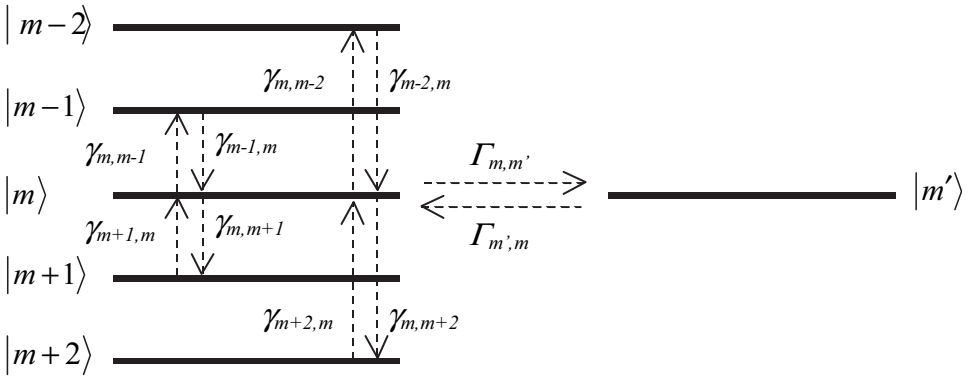

Figure 13 Schematic diagram of allowed transitions to or from level $|m\rangle$. Shown are first-order ($|m\rangle \leftrightarrow |m \pm 1\rangle$) and second-order ($|m\rangle \leftrightarrow |m \pm 2\rangle$) spin-phonon transitions as well as tunneling transitions ($|m\rangle \leftrightarrow |m'\rangle$).

The above discussion, while capturing some of the flavor of how the thermally assisted process works, is somewhat imprecise. Detailed theoretical analyses have been performed and I will review and contrast these now. The main differences among these theories are what

mechanisms produce tunneling and how the spin-phonon interaction is treated. Many of these theories take their cue from early work by Villain et al. [56], who treated the over-barrier (no tunneling) relaxation of molecular magnets. One of the first theoretical studies of the thermally assisted tunneling process was done by Garanin and Chudnovsky [87] (see also [7]). They treated the relaxation of Mn_{12} using a model of thermally assisted tunneling in which the tunneling is produced by a static transverse magnetic field, Eq. (5), and which included only first-order spin-phonon transitions, in which the coupling constant g_4 is calculated explicitly. They predict the resonance to be a superposition of Lorentzians, but the predicted relaxation rate was orders of magnitude too small and the line width was much narrower than that observed. They invoked inhomogeneous broadening by random fields to account for the broad resonances observed.

Luis *et al.* [96, 97] realized that although a transverse anisotropy (Eq. (4)) alone prohibits the odd resonances, by including a small transverse field, Eq. (5), one could get tunneling from all of the resonances. Put simply, the transverse field breaks the symmetry and lifts the selection rule while the transverse anisotropy is primarily responsible for the magnitude of the tunnel splittings. These authors also limit themselves to using first-order spin-phonon transitions, but treat the coupling constant as a free parameter in order to achieve satisfactory agreement between their calculated relaxation rate and the data. Their calculations also show an asymmetry between even and odd resonances that is not observed experimentally. The authors invoke inhomogeneous broadening to smooth their multiresonant results into a single peak [97]. Aside from their other limitations, since no inhomogeneous broadening was found experimentally (Fig. 12), these theories do not quantitatively explain the data.

Fort *et al.* [98] have offered a calculation of the resonance line shape that fits experimental data for the zero-field resonance reasonably well. Their calculation is based on the assumption that the tunneling is driven only by a fourth-order transverse anisotropy. As the authors note, this approach fails to account for the presence of the odd resonances. The new feature in their theory is the inclusion of second-order spin-phonon transitions. However, the second-order coupling constants g_1 and g_2 are treated as fitting parameters. Leuenberger and Loss [77, 78] attempted to redress this deficit by explicitly calculating one and estimating the other of these constants. With only one fitting parameter (the speed of sound), they were able to reasonably reproduce the relaxation rate, the shape and the width of the resonances. However, Chudnovsky and Garanin [100] have pointed out that the Leuenberger and Loss' derivation of the second-order spin-phonon coupling constants is erroneous. While conceding their mistake, Leuenberger and Loss argue [101] that their calculation of g_1 and g_2 nevertheless gives a reasonable estimate of these constants. Despite its flaws, Leuenberger and Loss' theory does appear to explain the measured line width of the resonances in Fig. 12. Although the data can be fit well by a Lorentzian, their theory predicts that the peak's width does not directly correspond to a level's lifetime. This is because the measurements only probe the tails of the levels' densities of states: At large values of bias $E_{m,m'}$, the ratio $r_m < 1$ and the bottleneck in the relaxation process is tunneling from $|m\rangle$ to $|m'\rangle$. However, when $E_{m,m'}$ becomes small enough so that $r_m > 1$, the relaxation bottleneck is thermal activation, which does not depend on the level's density of states. Thus, the observed line width cannot be simply equated with one specific microscopic time scale (inverse tunneling rate, level lifetime, etc.). In a recent calculation, Pohjola and Schoeller [99] obtain similar results to Leuenberger and Loss; but they argue that the width of the resonance peak represents the tunnel splitting.

Three of the above theoretical treatments [78, 96, 99] predict that the relaxation rate as a function of H should show very narrow satellite peaks next to the each of the main resonance peaks for $n \neq 0$. These satellite peaks are due to the fact (Eq. (3)) that for the same value of n different pairs of levels come into resonance at slightly different values of magnetic field. So, they represent tunneling through levels higher or lower than the dominant tunneling level pair. Most of the predicted satellite peaks are too narrow to be measured in realistic experiments. Nevertheless, in the thermally assisted tunneling regime some experiments [102] have seen extra peaks over a narrow range of temperature that agree qualitatively with the predictions. However, no quantitative explanation of the data currently exists. Another manifestation of this effect is seen in the crossover between thermally activated and pure quantum tunneling that I will discuss in Section IV.B.

At this point there seem to be two major obstacles to obtaining a detailed theoretical understanding of thermally assisted resonant tunneling process in Mn_{12}. The first is that it appears that the first-order spin-phonon transitions alone cannot explain the data. However, there are no first-principles calculations of the second-order coupling constants g_1 and g_2, and no measurements of them either. The second obstacle is that the transition rate depends crucially on the fourth-order transverse anisotropy, Eq. (4). The magnitude of the anisotropy parameter C has been estimated from high-field ESR [10] and inelastic-neutron-scattering (INS) [13] experiments. However, some recent high-resolution INS experiments [14, 103] have found that the magnitude of C may be as small as zero. A precise determination of this crucial parameter is essential for further progress.

There have been some theories that have attempted to explain the relaxation of Mn_{12} in terms of mechanisms other than tunneling. Burin, Prokof'ev and Stamp [104] have suggested that the relaxation can occur via dipolar flip-flop processes. This possibility has now been obviated by the aforementioned experiments that show that the resonant phenomenon is substantially unchanged when the molecules are dispersed in a glassy matrix and thereby have negligible dipole interactions [82]. Garg [105] has suggested that the relaxation may be due to a lattice distortion that occurs when levels are near resonance. This theory applies only to levels $|m = 1\rangle$ and $|m = -1\rangle$ and predicts that the effective barrier is reduced on resonance by about 10 mK, in contrast to the ac-susceptibility experiments that indicate that the barrier is reduced by as much as 12 K [62, 63].

III.D. Effects of Dipole and Hyperfine Fields; Hole-digging experiments

The Lorentzian line shape of the data in Fig. 12 indicates that the thermally assisted tunneling process is not inhomogeneously broadened by hyperfine fields, initially estimated to be 300 – 500 Oe [89]. So, where are the hyperfine fields? One possible resolution to this puzzle is offered by hole-digging experiments by Wernsdorfer et al. [106-108]. Before going into the details of these experiments, it is necessary to discuss the role of dipolar fields in the relaxation. I have mentioned already that dipole fields in Mn_{12} are too weak to provide the transverse fields necessary to produce tunneling. However, as noted in the discussion of Fig. 3, the dipolar interactions between molecules can have an effect on the relaxation because the field that any individual molecule sees comprises both the external field and the dipolar field due to all of its neighbors in the sample. Thus, for example, as a sample relaxes from some initial magnetization to its equilibrium

magnetization, the field the sample experiences is constantly evolving. A sample initially tuned to a resonant field may relax to the point where the mean field takes most of the molecules off resonance. This effect may be partially responsible for the non-exponential relaxation observed in Fig. 7. In fact, it has been checked by adding an oscillating component to the applied field with an amplitude larger than the resonance width [66]. The system is thus repeatedly brought back to the resonance condition, producing an overall increase in the relaxation rate compared to when the field is static.

Thomas et al. have reported [109] nonexponential relaxation for T > 2.0 K that they attribute to the fact that the mean dipolar field varies as the system relaxes. Their data, however, may also reflect the presence of a second species of Mn_{12} that relaxes faster (see below). The effect of dipolar fields on the relaxation of Fe_8 at milliKelvin temperatures has been studied by Ohm et al [110]. They found that the observed nonexponential relaxation in that system could be quantitatively explained using a simple model in which the distribution of dipole fields widens with time. Prokof'ev and Stamp [93, 94] have considered theoretically the role hyperfine and dipole fields play in the dynamics at low temperatures, where the relaxation proceeds exclusively via ground-state tunneling. Since the ground-state tunnel splitting is so small, the intrinsic resonance width is extremely narrow and any small longitudinal field will take a given molecule off of resonance, blocking the relaxation. In their model, each molecule sees both a small, rapidly varying hyperfine field and a quasistatic dipole field due to its neighbors. For a fraction of the molecules the net dipole field will happen to be small enough that the fluctuating hyperfine fields can sweep it through the resonance condition, allowing it to tunnel. Once it has tunneled, it alters the dipole fields seen by its neighbors, allowing some of them to tunnel, etc. Analyzing this process for a sample of ellipsoidal shape, they found that the magnetization of the sample should relax as $\sqrt{t}$ for short times *t*. It has been noted that $\sqrt{t}$ form of the relaxation does not actually require the presence of fluctuating fields [111] (see also [112, 113]). For other sample shapes, the precise form of the relaxation may be quite complicated, as has been investigated with Monte Carlo calculations [114]. Nevertheless, it has been found experimentally that at low temperatures and short times the relaxation for both Mn_{12} and Fe_8 follows t^{α} behavior with $\alpha \approx 0.3-0.5$ [106-108, 110, 113, 115].

The low-temperature relaxation in Mn_{12} is complicated by the existence of a second (minor) species of Mn_{12}, sometimes referred to as Mn_{12} (2). This minority species appears to be a distorted form of the majority Mn_{12} molecule and is randomly dispersed in the crystal [106, 116-118]. The resulting lower symmetry of the minority species results in a smaller effective energy barrier and concomitant faster relaxation rate. At low temperatures (T < 1 K), the primary species of Mn_{12} is completely frozen and only the relaxation of Mn_{12} (2) can be observed [106]. By measuring the slope of the short-time relaxation as a function of $\sqrt{t}$, Wernsdorfer et al. [106] determined a characteristic relaxation rate Γ_{sqrt} , which is plotted as a function of external field in Fig. 14a (open circles). This data represents the distribution of dipole fields seen by the Mn_{12} (2) molecules. Wernsdorfer et al. proceeded to dig a hole in this distribution through the following procedure. The system was cooled from 5 K to *T* < 1 K in zero field; then, a "hole-digging" field H_{dig} (arrow in Fig. 14a) was applied and the system was allowed to relax at this field for a time t_{dig} . During this time only those molecules that are near resonance at H_{dig} can tunnel. The field was then changed to a different value *H* and Γ_{sqrt} *(H)* was measured. This procedure was repeated

for several values of H to give each curve in Fig. 14a. One sees immediately that a hole has been dug into the distribution of dipole fields. This hole distribution is plotted in Fig. 14b. Wernsdorfer et al. found that the width of the hole becomes temperature independent below 400 mK and is approximately constant for $t_{dig} < 10$ s. Under these circumstances, the hole has a width of ~120 G.

They interpret this minimum width as a reflection of the distribution of the hyperfine fields. That is, depleting the distribution at H_{dig} can only affect the distribution at H only if $\left|H_{dig} - H\right| \leq H_{hyperfine}$. Following an analysis by Hartmann-Boutron et al. [89], they estimated that the hyperfine fields should have Gaussian full width of ~160 G, consistent with the measured hole width. Wernsdorfer et al. repeated their hole-digging procedure at high temperature (2 K), where the measured relaxation is dominated by the primary Mn_{12} species reversing via a thermally assisted process, and obtained a Lorentzian line shape, as in Fig. 12. However, they were unable to dig a hole into the high-temperature relaxation-rate distribution, indicating that high-temperature line shape does not represent the distribution of dipole fields, but rather has a dynamical significance. That is, it most likely reflects some aspect of the thermally assisted tunneling process, as discussed in the last subsection. Also, the fact that the resonance width found in that data is about twice the hole width may explain why no inhomogeneous broadening was found: such a small amount of hyperfine inhomogeneous broadening would not be discernable in the data shown in Fig. 12. It should be noted that the presence of rapidly fluctuating hyperfine fields at the mK temperatures of the hole-digging experiments is surprising. Proton NMR and μSR experiments [119, 120] suggest that the T_1 (longitudinal) relaxation time in Mn_{12} becomes exponentially slow at low temperature, comparable to the time for a phonon to be absorbed by the molecular spin. While the T_2 (transverse) relaxation time may be significantly faster, it is not entirely clear how such T_2 processes would alter the longitudinal field seen by the molecular spin.

Nevertheless, isotope effects provide evidence that the hole width is related to hyperfine fields. In Mn_{12}, one cannot readily investigate such isotope effects because there is only one stable isotope of Mn (with nuclear spin I = 5/2), which is undoubtedly the primary source of hyperfine fields seen by the molecule. In Fe_8, however, the situation is quite different, with 90% of Fe nuclei (^{56}Fe) having zero nuclear spin. Wernsdorfer et al. [107, 108] performed hole-digging experiments on Fe_8 and obtained qualitatively similar results to those in Mn_{12}. They studied three isotopically distinct samples of Fe_8: one with natural isotopic abundances, one enriched with ^{57}Fe (I = ½) that is expected to have larger hyperfine fields, and one in which the hyperfine fields are reduced by the substitution of deuterons for most of the protons. The measured hole widths confirm that the hole represents the hyperfine fields, with the ^{57}Fe-enriched sample having the largest hole width and the deuterated sample having the smallest. Another related effect is the observation [108, 121] that the tunneling rate appears to be somewhat faster for the ^{57}Fe-enriched sample and slower for the deuterated sample, as might be expected if the transverse hyperfine fields are to some degree helping to produce tunneling. If the observed isotope effect were not related to the hyperfine fields but rather the difference in nuclear mass, one would expect both isotopically modified samples to behave similarly since the nuclear masses in both are larger than in the natural sample.

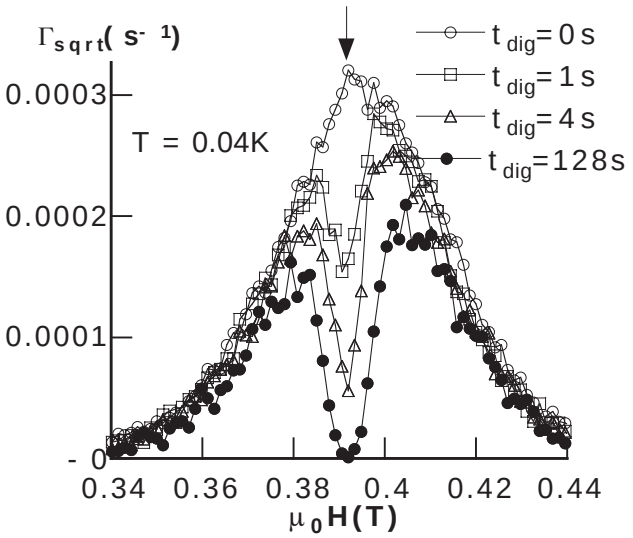

(a)

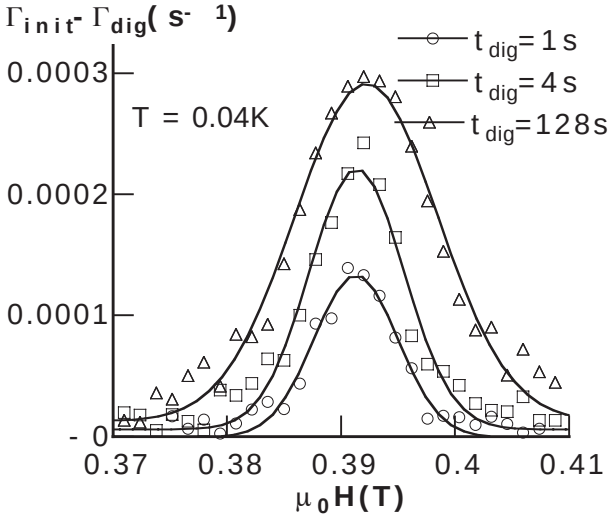

(b)

Figure 14 Hole-digging data for Mn_{12} at T = 0.04 K. (a) Square-root relaxation rate Γ_{sqrt} as a function of field H after the sample was first allowed to relax for a time t_{dig} at the field shown by the arrow. For $t_{dig} > 0$ a hole is dug into the curve. The hole, shown in (b), is interpreted as representing the fluctuating-hyperfine-field distribution. Reprinted with permission from W. Wernsdorfer, R. Sessoli and D. Gatteschi, Europhys. Lett. **47**, 254 (1999). Copyright 1999 EDP Sciences.

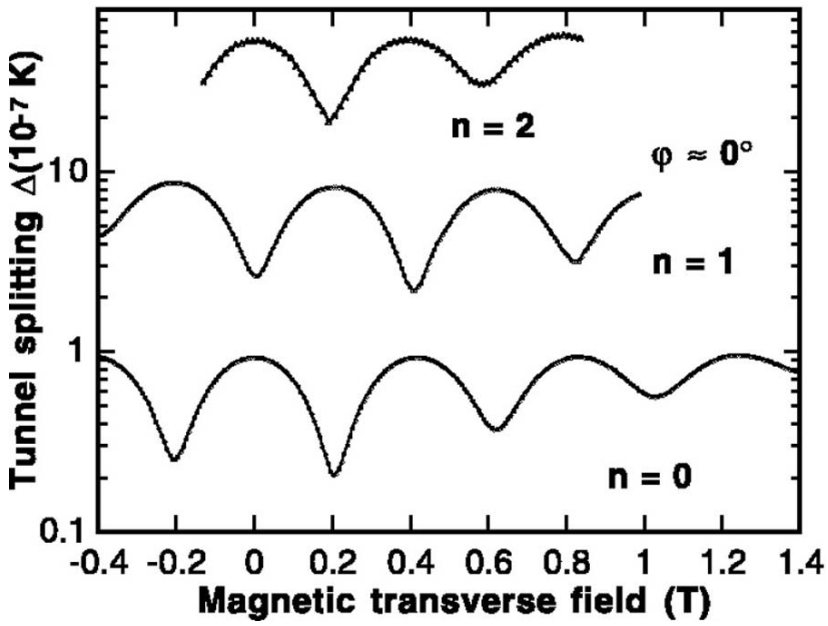

Figure 15 Measured tunnel splitting of Fe_8 as a function of the field H_x applied along the spin's hard axis. The tunnel splitting is reduced at the values of H_x for which the two minimal tunneling paths interfere destructively. Reprinted with permission from W. Wernsdorfer and R. Sessoli, Science **284**, 133 (1999). Copyright 1999 American Association for the Advancement of Science.

Let us summarize the main results of this section. First, because none of the tunneling resonances in Mn_{12} are missing or reduced, we can conclude that a selection rule has been violated and that the tunneling must by driven by a transverse magnetic field, most probably hyperfine fields. An externally applied transverse field does seem to augment the relaxation, but in a way that is not inconsistent with classical effects. A detailed study of the line shape of the zero-field resonance found no evidence of inhomogeneous broadening from a static hyperfine field distribution. Despite much theoretical work to understand the thermally assisted relaxation in Mn_{12}, the detailed dynamics are not yet understood, although it is clear that first-order spin-phonon coupling terms are not sufficient to explain the data. Finally, the hole-digging experiments have elucidated the role of hyperfine fields in the low-temperature relaxation.

IV. RECENT RESULTS

I will conclude this chapter by summarizing some of the most interesting recent experimental results found in the molecular magnets. In the beginning of this section I will discuss the quantum-phase-interference experiments of Wernsdorfer and Sessoli in which tunneling could be suppressed by the application of a transverse magnetic field. I will then briefly discuss the

observations of coherent quantum tunneling and of a "first-order" transition between thermally assisted tunneling and purely quantum tunneling.

IV.A. Quantum phase interference

The quantum-phase-interference phenomenon found by Wernsdorfer and Sessoli [121-123] is an example of a geometric-phase (Berry-phase) effect in which two tunneling paths interfere. The theory of this phenomenon is discussed in detail in Garg's contribution to this book. I will only briefly review the essential aspects here.

Let us consider the spin Hamiltonian

$$\mathcal{H} = -DS_z^2 + E(S_x^2 - S_y^2)\,, \tag{12}$$

where D > E > 0. The spin then has easy (z), medium (y) and hard (x) axes. If the spin is pointing along the z axis, it has two possible least-action tunneling (instanton) paths for reversal: one in which it passes through the positive y axis and one in which it passes through the negative y axis. The real part of the actions for these paths are equal, but for a spin S each path picks up a different geometric phase of

$$S\int(1-\cos\theta)d\phi\,, \tag{13}$$

where θ and ϕ are the usual polar and azimuthal angles, respectively, and the integral is taken over the instanton path. The path-dependent geometric phase leads to interference between the paths. The interference is completely destructive for half-integer *S*, leading to a complete suppression of tunneling in accordance with Kramers' theorem [124, 125].

It was pointed out by Garg [126, 127] that such a geometric-phase interference effect could be controlled by a transverse magnetic field with the tunnel splitting going to zero at regular intervals of field. This is a somewhat counterintuitive result since, as discussed in the last section, a transverse field tends to lower the classical energy barrier and hence increase tunneling. However, it should be noted that the effect is only possible if the field is oriented very nearly along the hard (*x*) axis. In that case, the Hamiltonian, Eq. (12), gains a term $-g\mu_B S_x H_x$, which moves the energy minima away from the poles and slightly towards the hard axis. The instanton paths no longer pass through the *y* axis. However, the symmetry between the two paths remains intact with each having the same real component to the instanton action, but a different geometric phase. Again, the paths can interfere, producing a tunnel splitting that is modulated by the factor $\cos(S\Theta)$, where Θ is the solid angle on the Bloch sphere circumscribed by the two paths. As the magnitude of the field is increased, Θ decreases and the tunnel splitting oscillates. Garg predicted that the tunnel splitting should go to zero at regular intervals of magnetic field with a period given by

$$\Delta H = \frac{2}{g\mu_B}\sqrt{2E(E+D)}\,. \tag{14}$$

Since Garg's original work, several other researchers have studied this effect theoretically [99, 128-136].

Before reviewing the experiments of Wernsdorfer and Sessoli that confirmed the geometric-phase interference effect, I will briefly discuss the features of the Fe_8 molecule that distinguish it from Mn_{12}. The chemical formula for Fe_8 is $(Fe_8O_2(OH)_{12}(tacn)_6)Br_8$, where *tacn* is 1,4,7-triazacyclononane, an organic ligand. Like Mn_{12}, the Fe_8 cluster has a spin of 10 [137]. It has a magnetocrystalline anisotropy barrier of ~22 K [137] and shows resonant tunneling effects (steps in the hysteresis loops) [138]. The system crystallizes into a triclinic lattice and thus has no non-trivial symmetry [137]. Nevertheless, the Fe core of the cluster has an approximate D_2 symmetry and the spin of the cluster has been found to be well described by Eq. (12) with D = -0.27 K and E = -0.046 K. (Like Mn_{12}, the Fe_8 Hamiltonian also contains fourth-order anisotropy terms, which do not affect the essential physics of the geometric-phase interference, but only some of the details.) As we have seen in Section III, in Mn_{12}, the off-diagonal terms in the Hamiltonian (those that do not commute with S_z) are small and have yet to be precisely pinned down. In Fe_8, however, the low symmetry allows for a substantial second-order transverse anisotropy term (the second term in Eq. (12)). This term is easily detected in ESR [76, 137] and INS [75] experiments, which yield an unambiguous value for E. Thus, "what causes tunneling" is pretty well understood for this system, although, as we shall see below, a transverse magnetic field must also be playing some role in the tunneling. The relatively large transverse anisotropy and small barrier allow tunneling from the ground state, so that at temperatures below 0.36 K this is the only mechanism for relaxation at all fields [138]. In contrast, as we have seen, in Mn_{12} tunneling is usually thermally assisted and occurs from excited states. (Ground-state tunneling can be seen in Mn_{12} at high magnetic fields – see below.)

In their experiments, Wernsdorfer and Sessoli [121-123] deduced the tunnel splitting for a particular resonance using a Landau-Zener tunneling method. Let us consider a system prepared in the $|m=-10\rangle$ state in a small negative field. If the field is then swept at a constant rate to a small positive value, this state will pass through resonance with $|m=10\rangle$. The probability of tunneling into the $|m=10\rangle$ state during this process is given by

$$P_{-10,10} = 1 - \exp\left(-\frac{\pi\Delta_{-10,10}^2}{4\hbar g \mu_B S dH/dt}\right), \tag{15}$$

where $\Delta_{-10,10}$ is the tunnel splitting between the two states (or, more properly, between the symmetric and antisymmetric superposition states). Similar expressions apply for other resonances, e.g. $|m=-10\rangle$ and $|m=9\rangle$. Now, this probability is simply proportional to the change in magnetization, i.e. the height of the step in the hysteresis loop. Thus, by measuring the height of a step* and knowing the field sweep rate *dH/dt*, Eq. (15) allows one to determine the tunnel splitting $\Delta_{-10,10}$ (or $\Delta_{-10,10-n}$ for other resonances). Wernsdorfer et al. [121, 123] checked

* In cases where the probability of tunneling P during a single sweep through the resonance was too small to measure, Wernsdorfer and Sessoli made multiple back-and-forth sweeps. The resulting transition probability P_N after N sweeps is then $P_N = NP$.

the validity of Eq. (15) as *dH/dt* was varied over several decades and found that it works when *dH/dt* > 10 Oe/s.

Using this method to determine the tunnel splitting Δ for each resonance, Wernsdorfer and Sessoli measured Δ as a function of transverse field H_x. The results, plotted in Fig. 15, show unmistakable oscillations Δ at three resonances n = 0, 1, 2. The tunnel splitting drops by nearly an order of magnitude at regular field intervals of 0.41 T. While this is qualitatively what is predicted by Eq. (14), it is nearly a factor of two larger than the numerical value derived from the equation. Wernsdorfer and Sessoli found that the measured field interval could be explained by including a transverse anisotropy term, i.e. Eq. (4), in the spin Hamiltonian for Fe_8.

One interesting feature of the data in Fig. 15 is that the odd resonance (n = 1) is out of phase with the even resonances (n = 0, 2). In particular, when $H_x = 0$, the tunnel splittings of the even resonances have maxima while the tunnel splitting of the odd resonance has a minimum. This is precisely the selection rule discussed in Section III.A that in the absence of a transverse field the odd resonances are forbidden. Why then is the tunnel splitting at n = 1 not much smaller? As in Mn_{12}, the presence of a small transverse field would lift the selection rule. In Fe_8 the hyperfine fields are much smaller than in Mn_{12}, but the dipole coupling between neighboring molecules is much larger, making the latter the likely source of the transverse field. Wernsdorfer et al. [121] showed that this is indeed the case by studying how Δ near the dip depends on the initial magnetization M_{in} of the sample. They found that as M_{in} is increased toward saturation, the dip gets sharper and deeper. For example, the tunnel splitting for the n = 1 resonance at $H_x = 0$ is about a factor of four smaller when $M_{in} = 0.098 M_{sat}$ than when $M_{in} = 0$. This is consistent with the idea that the dipole fields are the source of the transverse field since when the sample is near saturation, the "down" (unflipped) molecules see a nearly homogeneous longitudinal dipole field from all of "up" molecules. When $M_{in} = 0$, on the other hand, each "down" spin sees a random field from its neighbors that can have a substantial transverse component.

Thus, in these few experiments on the geometric-phase in Fe8, one can also see two additional interesting effects: the selection-rule suppression of tunneling (or "parity effect") and the effect of dipole fields on the tunnel splitting.

IV.B. Other recent results: Coherence and "First-order" transition

Some other recent results in the molecular magnets include the observation of quantum coherent tunneling and the discovery of a so-called "first-order" transition between thermally assisted tunneling and pure ground-state tunneling.

All of the tunneling phenomena presented thus far in this chapter have been incoherent: the system tunnels through the barrier and does not come back. This is because the relevant tunnel splitting Δ is usually small compared to the decoherence rate γ, e.g. the spin-phonon relaxation rate. Coherent tunneling occurs in the opposite limit when the decoherence rate is small and the system can then tunnel back and forth between the two wells such that probability of being found in, say, the left well varies as $\cos(\Delta t / \hbar)$. Equivalently, coherence means that the system can be put into a superposition of states on opposite sides of the barrier, e.g.

$|\pm\rangle = \frac{1}{\sqrt{2}}(|m=10\rangle \pm |m=-10\rangle)$; the energy difference between these two superposition states is the tunnel splitting $\Delta_{-10,10}$. For both Mn_{12} and Fe_8, this ground-state tunnel splitting is normally extremely small (cf. Fig. 14), leading to incoherent tunneling. But the ground-state tunneling can be augmented by applying a transverse magnetic field, as in the experiments discussed in Section III.B.

By applying a large transverse magnetic field to an oriented-powder sample of Fe_8, del Barco et al. [139] were able to increase the tunnel splitting of the ground state to the radio frequency range, enabling them to detect it directly via an ESR experiment. A subsequent experiment by Bellesa et al. [140] found a similar effect in Mn_{12}. In both experiments, the position of the detected spectral peaks could be predicted from the relevant spin Hamiltonian with no adjustable parameters. The trick in these experiments was the use of a powdered sample. In order to observe the coherent state, the magnetic field must be nearly perfectly perpendicular to the molecule's easy axis. A small longitudinal component to the field will tilt the potential and localize the two states in different wells with negligible coupling between them. This difficulty is overcome by using a powdered sample: most of the molecules will be misaligned with the field, but they will contribute no signal; only the small fraction for which the field is nearly perpendicular will exhibit a resonance signal.

Another aspect of ground-state tunneling is the question of how, as temperature is lowered, a system makes a transition between thermally assisted tunneling and pure quantum tunneling. Chudnovsky [141] predicted theoretically that the crossover could either be a sudden, "first-order" or a smooth, "second-order" transition, depending on the curvature of the potential barrier. Most tunneling systems of experimental interest, such as the SQUID system discussed in Han's chapter, have a potential shape that always gives rise to a second-order transition. Chudnovsky and Garanin [87, 142] showed that a uniaxial spin, such as Mn_{12}, can have a first-order transition, and, furthermore, the transition can be made second order by the application of a suitably large transverse magnetic field. Many aspects of this effect have been explored theoretically since this prediction [143-151].

A simple way to understand the meaning of a first-order transition is to return to the analysis in Section III.C of the thermally assisted tunneling process. There I argued that for any given temperature, there is almost always one pair of tunneling levels that dominates the relaxation process, the lowest pair for which $r_m < 1$ (see Eq. (11)). As the temperature is lowered, the dominant pair will fall from one pair of levels to a pair below it and eventually, at very low temperatures, tunneling will only occur from the ground state. If this process of climbing down the ladder of levels occurs smoothly from one pair to the next (i.e. from m = 8 to 9 to 10) as the temperature is lowered, then it is a second-order transition. However, if some of the lowest levels are rapidly skipped (i.e. going directly from m = 8 to 10), then the transition to ground-state tunneling is first order.

This signature of skipping levels is exactly what was found by Kent et al. [152, 153] in studying Mn_{12} at large values of n (= 5 – 9), where the potential is significantly tilted and barrier reduced. They could identify which levels participated in the tunneling because for a given value of n, the resonance field, Eq. (3), depends on values of m and m' because of the presence of the fourth-order anisotropy. As the temperature was lowered, they found that the field at which a step occurs in the hysteresis loop increases smoothly but then makes a sudden jump at $T \approx 1.0K$ when the system crosses over to ground-state tunneling. A careful analysis, as well as some detailed subsequent work by Mertes et al. [154], shows that this sudden jump corresponds to a transition

from thermally assisted tunneling from $m = 8$ to ground-state tunneling from $m = 10$, skipping $m = 9$. At temperatures below this crossover, both the position of the resonant step and the relaxation rate are temperature independent, confirming that tunneling is occurring from the ground state.

By applying a transverse field, Bokacheva et al. [155] were able to smooth out the crossover to ground-state tunneling, i.e. making it a second-order transition, in qualitative accord with the predictions of Chudnovsky and Garanin [142]. Interestingly, another group [156] simultaneously published an experimental report in which they claim that the transition is always second order. The discrepancy has not been explained. Another interesting result is that Fe_8, in contrast to Mn_{12}, seems to exhibit a smooth, second-order transition to ground-state tunneling [123]. This fact appears to be related to the existence of a second-order transverse anisotropy in the molecule's spin Hamiltonian, Eq. (12), and has been addressed theoretically [157].

V. SUMMARY AND OUTLOOK

I began this chapter by noting that spin systems are significantly different from other tunneling systems. I hope the reader has found that the molecular magnets exhibit a rich set of phenomena, from resonant tunneling to geometric-phase interference, and raise some interesting fundamental questions, like "What causes tunneling?", that exemplify the uniqueness of magnetization tunneling.

I want to emphasize that, while much is known about the relaxation process in the molecular magnets, many details still remain to be discerned. Some of the outstanding questions include the nature of the spin-phonon interaction, the role of hyperfine and dipole fields, and how the dominant tunneling pair changes as temperature or transverse magnetic field are varied. All of these questions have been addressed to some degree or another and there is no doubt that further progress is to come.

I would like to acknowledge the contributions of my numerous collaborators, including Myriam Sarachik, Eugene Chudnovsky, Javier Tejada, Ron Ziolo, Joan Manel Hernández, Xixiang Zhang, Rob Robinson, Yicheng Zhong, Tim Kelley, Heinz Nakotte, Frans Trouw, Wei Bao, Sheila Aubin and Dave Hendrickson. I am also indebted to Wolfgang Wernsdorfer, Roberta Sessoli, Daniel Loss, Nikolay Prokof'ev, Philip Stamp for useful discussions about their work. Finally, I would like to thank my wife Teresa Buswell for her support.

REFERENCES

[1] H. Grabert and U. Weiss, Phys. Rev. Lett. **53**, 1787 (1984).
[2] U. Weiss, H. Grabert and S. Linkwitz, J. Low Temp. Phys. **68**, 213 (1987).
[3] A. J. Leggett, S. Chakravarty, A. T. Dorsey, M. P. A. Fisher, A. Garg and W. Zwerger, Rev. Mod. Phys. **59**, 1 (1987).
[4] J. R. Friedman, M. P. Sarachik, J. Tejada, J. Maciejewski and R. Ziolo, J. Appl. Phys. **79**, 6031 (1996).
[5] J. R. Friedman, M. P. Sarachik, J. Tejada and R. Ziolo, Phys. Rev. Lett. **76**, 3830 (1996).

[6] J. M. Hernández, X. X. Zhang, F. Luis, J. Tejada, J. R. Friedman, M. P. Sarachik and R. Ziolo, Phys. Rev. B **55**, 5858 (1997).
[7] J. R. Friedman, Ph.D. thesis (The City University of New York, New York, 1996).
[8] A. Caneschi, D. Gatteschi, C. Sangregorio, R. Sessoli, L. Sorace, A. Cornia, M. A. Novak, C. Paulsen and W. Wernsdorfer, J. Magn. Magn. Mat. **200**, 182 (1999).
[9] B. Barbara, L. Thomas, F. Lionti, I. Chiorescu and A. Sulpice, J. Magn. Magn. Mat. **200**, 167 (1999).
[10] A. L. Barra, D. Gatteschi and R. Sessoli, Phys. Rev. B **56**, 8192 (1997).
[11] S. Hill, J. A. A. J. Perenboom, N. S. Dalal, T. Hathaway, T. Stalcup and J. S. Brooks, Phys. Rev. Lett. **80**, 2453 (1998).
[12] A. A. Mukhin, V. D. Travkin, A. K. Zvezdin, S. P. Lebedev, A. Caneschi and D. Gatteschi, Europhys. Lett. **44**, 778 (1998).
[13] I. Mirebeau, M. Hennion, H. Casalta, H. Andres, H. U. Güdel, A. V. Irodova and A. Caneschi, Phys. Rev. Lett. **83**, 628 (1999).
[14] W. Bao, R. A. Robinson, J. R. Friedman, H. Casalta, E. Rumberger and D. N. Hendrickson, cond-mat/0008042 (2000).
[15] A. O. Caldeira and A. J. Leggett, Phys. Rev. Lett. **46**, 211 (1981).
[16] A. O. Caldeira and A. J. Leggett, Ann. Phys. (N.Y.) **149**, 374 (1983).
[17] J. Clarke, A. N. Cleland, M. H. Devoret, D. Esteve and J. M. Martinis, Science **239**, 992 (1988).
[18] C. P. Bean and J. D. Livingston, J. Appl. Phys. **30**, 120S (1959).
[19] T. Egami, Phys. Status Solidi **A 20**, 157 (1973).
[20] B. Barbara, G. Fillion, D. Gignoux and R. Lemaire, Solid State Comm. **10**, 1149 (1973).
[21] O. Bostanjoglo and H. P. Gemund, Phys. Status Solidi **A 17**, 115 (1973).
[22] O. Bostanjoglo and H. P. Gemund, Phys. Status Solidi **A 48**, 41 (1978).
[23] J. A. Baldwin, F. Milstein, R. C. Wong and J. L. West, J. Appl. Phys. **48**, 2612 (1977).
[24] W. Reihemann and E. Nembach, J. Appl. Phys. **55**, 1081 (1984).
[25] W. Reihemann and E. Nembach, J. Appl. Phys. **57**, 476 (1986).
[26] M. Enz and R. Schilling, J. Phys. C: Solid State Phys. **19**, 1765 (1986).
[27] J. L. van Hemmen and A. Süto, Europhys. Lett. **1**, 481 (1986).
[28] E. M. Chudnovsky and L. Gunther, Phys. Rev. Lett. **60**, 661 (1988).
[29] P. C. E. Stamp, E. M. Chudnovsky and B. Barbara, Int. J. Mod. Phys. B **6**, 1355 (1992).
[30] R. Schilling, in *Quantum Tunneling of Magnetization*, edited by L. Gunther and B. Barbara (Kluwer, Amsterdam, 1995).
[31] J. L. van Hemmen and A. Süto, in *Quantum Tunneling of Magnetization*, edited by L. Gunther and B. Barbara (Kluwer, Amsterdam, 1995).
[32] E. M. Chudnovsky and J. Tejada, *Macroscopic Quantum Tunneling of the Magnetic Moment* (Cambridge University Press, Cambridge, 1998).
[33] A. Garg and G. H. Kim, Phys. Rev. Lett. **63**, 2512 (1989).
[34] A. Garg and G. H. Kim, J. Appl. Phys. **67**, 5669 (1990).
[35] B. Barbara, L. C. Sampaio, J. E. Wegrowe, B. A. Ratnam, A. Marchand, C. Paulsen, M. A. Novak, J. L. Tholence, M. Uehara and D. Fruchart, J. Appl. Phys. **73**, 6703 (1993).
[36] B. Barbara, W. Wernsdorfer, L. C. Sampaio, J. G. Park, C. Paulsen, M. A. Novak, R. Ferré, D. Mailly, R. Sessoli, A. Caneschi, K. Hasselbach, A. Benoit and L. Thomas, J. Magn. Magn. Mater. **140-144**, 1825 (1995).
[37] J. Tejada and X. X. Zhang, J. Appl. Phys. **73**, 6709 (1995).

[38] D. D. Awschalom, D. P. DiVincenzo and J. F. Smyth, Science **258**, 414 (1992).
[39] E. M. Chudnovsky, Science **274**, 938 (1996).
[40] A. Garg, Phys. Rev. Lett. **70**, 2198 (1993).
[41] D. D. Awschalom, J. F. Smyth, G. Grinstein, D. P. DiVincenzo and D. Loss, Phys. Rev. Lett. **70**, 2199 (1993).
[42] A. Garg, Phys. Rev. Lett. **71**, 4249 (1993).
[43] D. D. Awschalom, D. P. DiVincenzo, G. Grinstein and D. Loss, Phys. Rev. Lett. **71** (1993).
[44] J. Tejada, Science **272**, 424 (1996).
[45] T. Lis, Acta Cryst. B **36**, 2042 (1980).
[46] C. Paulsen, J.-G. Park, B. Barbara, R. Sessoli and A. Caneschi, J. Magn. Magn. Mater. **140-144**, 379 (1995).
[47] M. A. Novak, R. Sessoli, A. Caneschi and D. Gatteschi, J. Magn. Magn. Mater. **146**, 211 (1995).
[48] M. A. Novak and R. Sessoli, in *Quantum Tunneling of Magnetization*, edited by L. Gunther and B. Barbara (Kluwer, Dordrecht, 1995), p. 171.
[49] C. Paulsen and J.-G. Park, in *Quantum Tunneling of Magnetization*, edited by L. Gunther and B. Barbara (Kluwer, Dordrecht, 1995), p. 189.
[50] M. Hennion, L. Pardi, I. Mirebeau, E. Suard, R. Sessoli and A. Caneschi, Phys. Rev. B **56**, 8819 (1997).
[51] M. I. Katsnelson, V. V. Dobrovitski and B. N. Harmon, Phys. Rev. B **59**, 6919 (1999).
[52] M. I. Katsnelson, V. V. Dobrovitski and B. N. Harmon, J. Appl. Phys. **85**, 4533 (1999).
[53] M. Al-Saqer, V. V. Dobrovitski, B. N. Harmon and M. I. Katsnelson, J. Appl. Phys. **87**, 6268 (2000).
[54] A. Caneschi, D. Gatteschi, R. Sessoli, A. L. Barra, L. C. Brunel and M. Guillot, J. Am. Chem. Soc. **113**, 5873 (1991).
[55] R. Sessoli, H.-L. Tsai, A. R. Schake, S. Wang, J. B. Vincent, K. Folting, D. Gatteschi, G. Christou and D. N. Hendrickson, J. Am. Chem. Soc. **115**, 1804 (1993).
[56] J. Villain, F. Hartmann-Boutron, R. Sessoli and A. Rettori, Europhys. Lett. **27**, 159 (1994).
[57] R. A. Robinson, P. J. Brown, D. N. Argyriou, D. N. Hendrickson and S. M. J. Aubin, J. Phys. - Condens. Mat. **12**, 2805 (2000).
[58] Z. Zeng, D. Guenzburger and D. E. Ellis, Phys. Rev. B **59**, 6927 (1999).
[59] R. Sessoli, D. Gatteschi, A. Caneschi and M. A. Novak, Nature **365**, 141 (1993).
[60] R. Sessoli, Mol. Cryst. Liq. Cryst. **274**, A 145 (1995).
[61] H. J. Eppley, S. M. J. Aubin, M. W. Wemple, D. M. Adams, H. L. Tsai, V. A. Grillo, S. L. Castro, Z. M. Sun, K. Folting, J. C. Huffman, D. N. Hendrickson and G. Christou, Mol. Cryst. Liq. Cryst. Sci. Technol. Sect. A-Mol. Cryst. Liq. Cryst. **305**, 167 (1997).
[62] A. M. Gomes, M. A. Novak, R. Sessoli, A. Caneschi and D. Gatteschi, Phys. Rev. B **57**, 5021 (1998).
[63] F. Luis, J. Bartolomé, J. F. Fernández, J. Tejada, J. M. Hernández, X. X. Zhang and R. Ziolo, Phys. Rev. B **55**, 11448 (1997).
[64] J. M. Hernández, X. X. Zhang, F. Luis, J. Bartolomé, J. Tejada and R. Ziolo, Europhys. Lett. **35**, 301 (1996).
[65] L. Thomas, F. Lionti, R. Ballou, D. Gatteschi, R. Sessoli and B. Barbara, Nature **383**, 145 (1996).

[66] J. A. A. J. Perenboom, J. S. Brooks, S. Hill, T. Hathaway and N. S. Dalal, Phys. Rev. B **58**, 330 (1998).
[67] F. Fominaya, J. Villain, P. Gandit, J. Chaussy and A. Caneschi, Phys. Rev. Lett. **79**, 1126 (1997).
[68] J. F. Fernández, F. Luis and J. Bartolomé, Phys. Rev. Lett. **80**, 5659 (1998).
[69] M. Sales, J. M. Hernández, J. Tejada and J. L. Martínez, Phys. Rev. B **60**, 14557 (1999).
[70] Z. H. Jang, A. Lascialfari, F. Borsa and D. Gatteschi, Phys. Rev. Lett. **84**, 2977 (2000).
[71] R. Sessoli, private communication (1998).
[72] J. R. Friedman, unpublished (1998).
[73] S. Foner, private communication (1996).
[74] Y. C. Zhong, M. P. Sarachik, J. R. Friedman, R. A. Robinson, T. M. Kelley, H. Nakotte, A. C. Christianson, F. Trouw, S. M. J. Aubin and D. N. Hendrickson, J. Appl. Phys. **85**, 5636 (1999).
[75] R. Caciuffo, C. Amoretti, A. Murani, R. Sessoli, A. Caneschi and D. Gatteschi, Phys. Rev. Lett. **81**, 4744 (1998).
[76] A. L. Barra, D. Gatteschi and R. Sessoli, Chem. Eur. J. **6**, 1608 (2000).
[77] M. N. Leuenberger and D. Loss, Europhys. Lett. **46**, 692 (1999).
[78] M. N. Leuenberger and D. Loss, Phys. Rev. B **61**, 1286 (2000).
[79] S. M. J. Aubin, N. R. Dilley, M. W. Wemple, M. B. Maple, G. Christou and D. N. Hendrickson, J. Am. Chem. Soc. **120**, 839 (1998).
[80] S. M. J. Aubin, Z. Sun, L. Pardi, J. Krzystek, K. Folting, L.-C. Brunel, A. L. Rheingold, G. Christou and D. N. Hendrickson, Inorg. Chem. **38**, 5329 (1999).
[81] S. M. J. Aubin, N. R. Dilley, L. Pardi, J. Krzystek, M. W. Wemple, L. C. Brunel, M. B. Maple, G. Christou and D. N. Hendrickson, J. Am. Chem. Soc. **120**, 4991 (1998).
[82] A. Caneschi, T. Ohm, C. Paulsen, D. Rovai, C. Sangregorio and R. Sessoli, J. Magn. Magn. Mater. **177-181**, 1330 (1998).
[83] J. R. Friedman, M. P. Sarachik, J. M. Hernández, X. X. Zhang, J. Tejada, E. Molins and R. Ziolo, J. Appl. Phys. **81**, 3978 (1997).
[84] F. Lionti, L. Thomas, R. Ballou, B. Barbara, A. Sulpice, R. Sessoli and D. Gatteschi, J. Appl. Phys. **81**, 4608 (1997).
[85] J. R. Friedman and E. M. Chudnovsky, unpublished (1996).
[86] J. R. Friedman, Phys. Rev. B **57**, 10291 (1998).
[87] D. A. Garanin and E. M. Chudnovsky, Phys. Rev. B **56**, 11102 (1997).
[88] I. Y. Korenblit and E. F. Shender, Sov. Phys. JETP **48**, 937 (1978).
[89] F. Hartmann-Boutron, P. Politi and J. Villain, Int. J. Mod. Phys. **10**, 2577 (1996).
[90] J. R. Friedman, M. P. Sarachik and R. Ziolo, Phys. Rev. B **58**, R14729 (1998).
[91] V. V. Dobrovitski and A. K. Zvezdin, Europhys. Lett. **38**, 377 (1997).
[92] L. Gunther, Europhys. Lett. **39**, 1 (1997).
[93] N. V. Prokof'ev and P. C. E. Stamp, J. Low. Temp. Phys. **104**, 143 (1996).
[94] N. V. Prokof'ev and P. C. E. Stamp, Phys. Rev. Lett. **80**, 5794 (1998).
[95] K. Saito, S. Miyashita and H. D. Raedt, Phys. Rev. B **60**, 14553 (1999).
[96] F. Luis, J. Bartolomé and J. F. Fernández, Phys. Rev. B **57**, 505 (1998).
[97] J. F. Fernández, J. Bartolomé and F. Luis, J. Appl. Phys. **83**, 6940 (1998).
[98] A. Fort, A. Rettori, J. Villain, D. Gatteschi and R. Sessoli, Phys. Rev. Lett. **80**, 612 (1998).
[99] T. Pohjola and H. Schoeller, Physical Review B **62**, 15026 (2000).

[100] G. H. Kim and E. M. Chudnovsky, Europhys. Lett. **52**, 681 (2000).
[101] M. N. Leuenberger and D. Loss, Europhys. Lett. **52**, 247 (2000).
[102] Y. Zhong, M. P. Sarachik, J. Yoo and D. N. Hendrickson, Physical Review B **62**, R9256 (2000).
[103] I. Mirebeau, M. Hennion, H. Casalta, H. Andres, H. U. Güdel, A. V. Irodova and A. Caneschi, cond-mat/0009233 (2000).
[104] A. L. Burin, N. V. Prokof'ev and P. C. E. Stamp, Phys. Rev. Lett. **76**, 3040 (1996).
[105] A. Garg, Phys. Rev. Lett. **81**, 1513 (1998).
[106] W. Wernsdorfer, R. Sessoli and D. Gatteschi, Europhys. Lett. **47**, 254 (1999).
[107] W. Wernsdorfer, T. Ohm, C. Sangregorio, R. Sessoli, D. Mailly and C. Paulsen, Phys. Rev. Lett. **82**, 3903 (1999).
[108] W. Wernsdorfer, A. Caneschi, R. Sessoli, D. Gatteschi, A. Cornia, V. Villar and C. Paulsen, Phys. Rev. Lett. **84**, 2965 (2000).
[109] L. Thomas, A. Caneschi and B. Barbara, Phys. Rev. Lett. **83**, 2398 (1999).
[110] T. Ohm, C. Sangregorio and C. Paulsen, Eur. Phys. J. B. **6**, 195 (1998).
[111] E. M. Chudnovsky, Phys. Rev. Lett. **84**, 5676 (2000).
[112] N. V. Prokof'ev and P. C. E. Stamp, Phys. Rev. Lett. **84**, 5677 (2000).
[113] W. Wernsdorfer, C. Paulsen and R. Sessoli, Phys. Rev. Lett. **84**, 5678 (2000).
[114] A. Cuccoli, A. Fort, A. Rettori, E. Adam and J. Villain, Eur. Phys. J. B **12**, 39 (1999).
[115] T. Ohm, C. Sangregorio and C. Paulsen, J. Low Temp. Phys. **113**, 1141 (1998).
[116] S. M. J. Aubin, Z. Sun, I. A. Guzei, A. L. Rheingold, G. Christou and D. N. Hendrickson, Chemical Communications, 2239 (1997).
[117] Z. Sun, D. Ruiz, E. Rumberger, C. D. Incarvito, K. Folting, A. L. Rheingold, G. Christou and D. N. Hendrickson, Inorganic Chemistry **37**, 4758 (1998).
[118] Z. Sun, D. Ruiz, N. R. Dilley, M. Soler, J. Ribas, K. Folting, M. B. Maple, G. Christou and D. N. Hendrickson, Chem. Commun., 1973 (1999).
[119] A. Lascialfari, D. Gatteschi, F. Borsa, A. Shastri, Z. H. Jang and P. Carretta, Phys. Rev. B **57**, 514 (1998).
[120] A. Lascialfari, Z. H. Jang, F. Borsa, P. Carretta and D. Gatteschi, Phys. Rev. Lett. **81**, 3773 (1998).
[121] W. Wernsdorfer, R. Sessoli, A. Caneschi, D. Gatteschi, A. Cornia and D. Mailly, J. Appl. Phys. **87**, 5481 (2000).
[122] W. Wernsdorfer and R. Sessoli, Science **284**, 133 (1999).
[123] W. Wernsdorfer, R. Sessoli, A. Caneschi, D. Gatteschi and A. Cornia, Europhys. Lett. **50**, 552 (2000).
[124] D. Loss, D. P. DiVincenzo and G. Grinstein, Phys. Rev. Lett. **69**, 3232 (1992).
[125] J. von Delft and C. L. Henley, Phys. Rev. Lett. **69**, 3236 (1992).
[126] A. Garg, Europhys. Lett. **22**, 205 (1993).
[127] A. Garg, Phys. Rev. B **51**, 15161 (1995).
[128] S. E. Barnes, J. Phys.-Condes. Matter **10**, L665 (1998).
[129] R. Lu, J. L. Zhu, X. Chen and L. Chang, Eur. Phys. J. B **3**, 35 (1998).
[130] A. Garg, Phys. Rev. B **60**, 6705 (1999).
[131] A. Garg, Phys. Rev. Lett. **83**, 4385 (1999).
[132] G. H. Kim, Phys. Rev. B **60**, R3728 (1999).
[133] R. Lu, J. L. Zhu, X. B. Wang and L. Chang, Phys. Rev. B **60**, 4101 (1999).
[134] E. M. Chudnovsky and X. Martinez-Hidalgo, Europhys. Lett. **50**, 395 (2000).

[135] A. Garg, Europhys. Lett. **50**, 382 (2000).
[136] S. Y. Lee and S. K. Yoo, Phys. Rev. B **62**, 13884 (2000).
[137] A.-L. Barra, P. Debrunner, D. Gatteschi, C. E. Schulz and R. Sessoli, Europhys. Lett. **35**, 133 (1996).
[138] C. Sangregorio, T. Ohm, C. Paulsen, R. Sessoli and D. Gatteschi, Phys. Rev. Lett. **78**, 4645 (1997).
[139] E. del Barco, N. Vernier, J. M. Hernandez, J. Tejada, E. M. Chudnovsky, E. Molins and G. Bellessa, Europhys. Lett. **47**, 722 (1999).
[140] G. Bellessa, N. Vernier, B. Barbara and D. Gatteschi, Phys. Rev. Lett. **83**, 416 (1999).
[141] E. M. Chudnovsky, Phys. Rev. A **46**, 8011 (1992).
[142] E. M. Chudnovsky and D. A. Garanin, Phys. Rev. Lett. **79**, 4469 (1997).
[143] D. A. Garanin, X. M. Hidalgo and E. M. Chudnovsky, Phys. Rev. B **57**, 13639 (1998).
[144] J. Q. Liang, H. J. W. Muller-Kirsten, D. K. Park and F. Zimmerschied, Phys. Rev. Lett. **81**, 216 (1998).
[145] S. Y. Lee, H. J. W. Muller-Kirsten, D. K. Park and F. Zimmerschied, Phys. Rev. B **58**, 5554 (1998).
[146] D. A. Garanin and E. M. Chudnovsky, Phys. Rev. B **59**, 3671 (1999).
[147] S. P. Kou, J. Q. Liang, Y. B. Zhang, X. B. Wang and F. C. Pu, Phys. Rev. B **59**, 6309 (1999).
[148] G. H. Kim, Phys. Rev. B **59**, 11847 (1999).
[149] C. S. Park, S. K. Yoo, D. K. Park and D. H. Yoon, Phys. Rev. B **59**, 13581 (1999).
[150] G. H. Kim, J. Appl. Phys. **86**, 1062 (1999).
[151] G. H. Kim, Europhys. Lett. **51**, 216 (2000).
[152] A. D. Kent, Y. C. Zhong, L. Bokacheva, D. Ruiz, D. N. Hendrickson and M. P. Sarachik, Europhys. Lett. **49**, 521 (2000).
[153] A. D. Kent, Y. C. Zhong, L. Bokacheva, D. Ruiz, D. N. Hendrickson and M. P. Sarachik, J. Appl. Phys. **87**, 5493 (2000).
[154] K. M. Mertes, Y. Zhong, M. P. Sarachik, Y. Paltiel, H. Shtrikman, E. Zeldov, E. Rumberger and D. N. Hendrickson, cond-mat/0012247 (2000).
[155] L. Bokacheva, A. D. Kent and M. A. Walters, Phys. Rev. Lett. **85**, 4803 (2000).
[156] I. Chiorescu, R. Giraud, A. G. M. Jansen, A. Caneschi and B. Barbara, Phys. Rev. Lett. **85**, 4807 (2000).
[157] D. A. Garanin and E. M. Chudnovsky, Phys. Rev. B **6302**, 4418 (2001).